CO_2 og karbonbudsjettet

Betydning for klima og klimaendringer

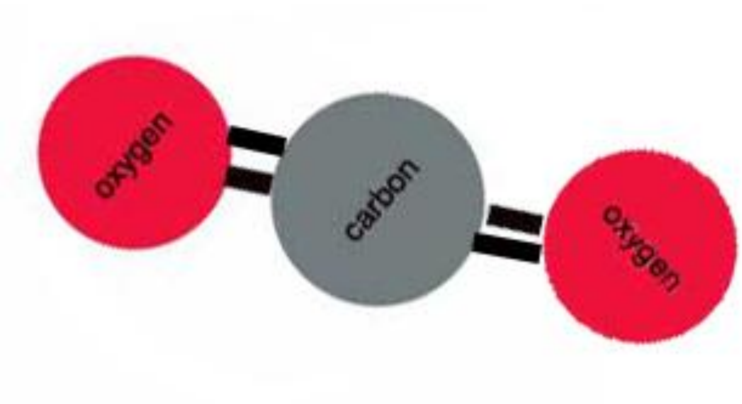

Hvorfor er CO_2 viktig som drivhusgass?

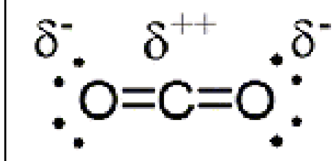

TABLE 1.2. The most important atmospheric constituents. The chlorofluorocarbons (CFCs) CCl_2F_2 and CCl_3F are also known as CFC12 and CFC11, respectively. [N.B. (ppm, ppb, ppt) = parts per (million, billion, trillion)] The concentrations of some constituents are increasing systematically because of human activity. For example, the CO_2 concentration of 380 ppm was measured in 2004 (see Fig. 1.3); CFCs are now decreasing in concentration following restrictions on their production.

Chemical species	Molecular weight (g mol^{-1})	Proportion by volume	Chemical species	Molecular weight	Proportion by volume
N_2	28.01	78%	O_3	48.00	~500 ppb
O_2	32.00	21%	N_2O	44.01	310 ppb
Ar	39.95	0.93%	CO	28.01	120 ppb
H_2O (vapor)	18.02	~0.5%	NH_3	17.03	~100 ppb
CO_2	44.01	380 ppm	NO_2	46.00	~1 ppb
Ne	20.18	19 ppm	CCl_2F_2	120.91	480 ppt
He	4.00	5.2 ppm	CCl_3F	137.37	280 ppt
CH_4	16.04	1.7 ppm	SO_2	64.06	~200 ppt
Kr	83.8	1.1 ppm	H_2S	34.08	~200 ppt
H_2	2.02	~500 ppb	AIR	28.97	

TABLE 1.2. The most important atmospheric constituents. The chlorofluorocarbons (CFCs) CCl_2F_2 and CCl_3F are also known as CFC-12 and CFC-11, respectively. [N.B. (ppm, ppb, ppt) = parts per (million, billion, trillion)] The concentrations of some constituents are increasing systematically because of human activity. For example, the CO_2 concentration of 380 ppm was measured in 2004 (see Fig. 1.3); CFCs are now decreasing in concentration following restrictions on their production.

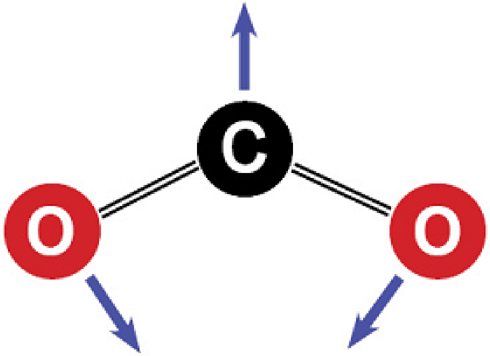

Carbon dioxide molecule. The arrows show how the molecule vibrates when it absorbs energy.

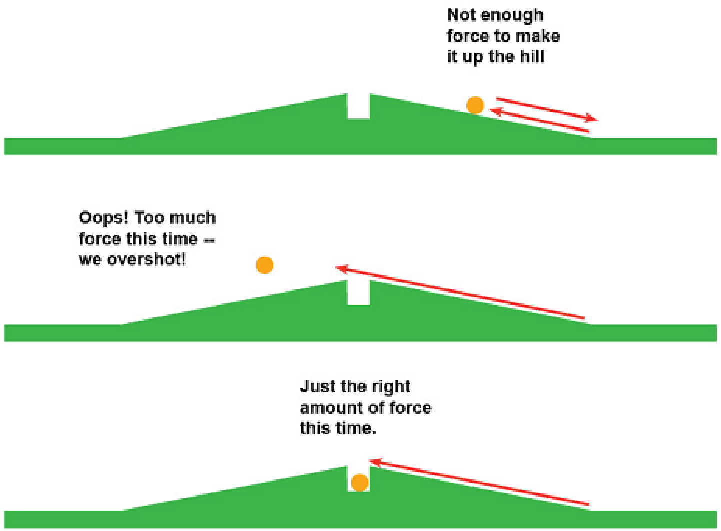

N_2, O_2 og edelgasser: Har ikke dipolmoment

➔ Disse er ikke drivhusgasser

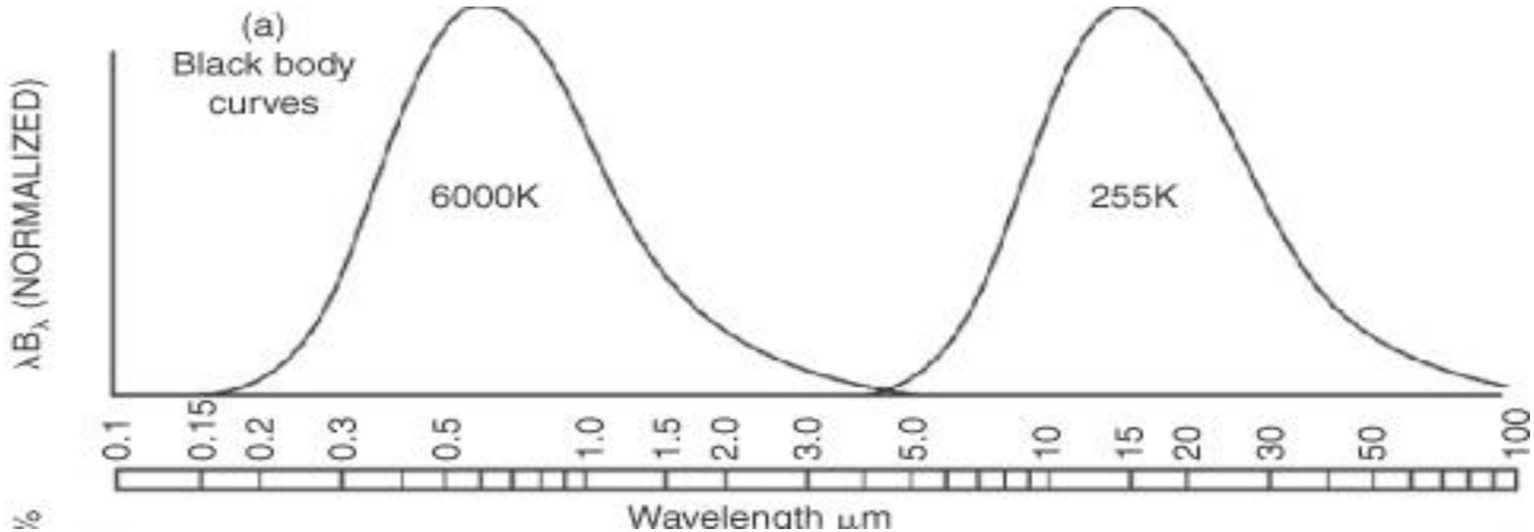

Svartlegemestråling fra legemer med temperatur:

- 6000K (Sola)
- 255K (Jordas atmosfære)

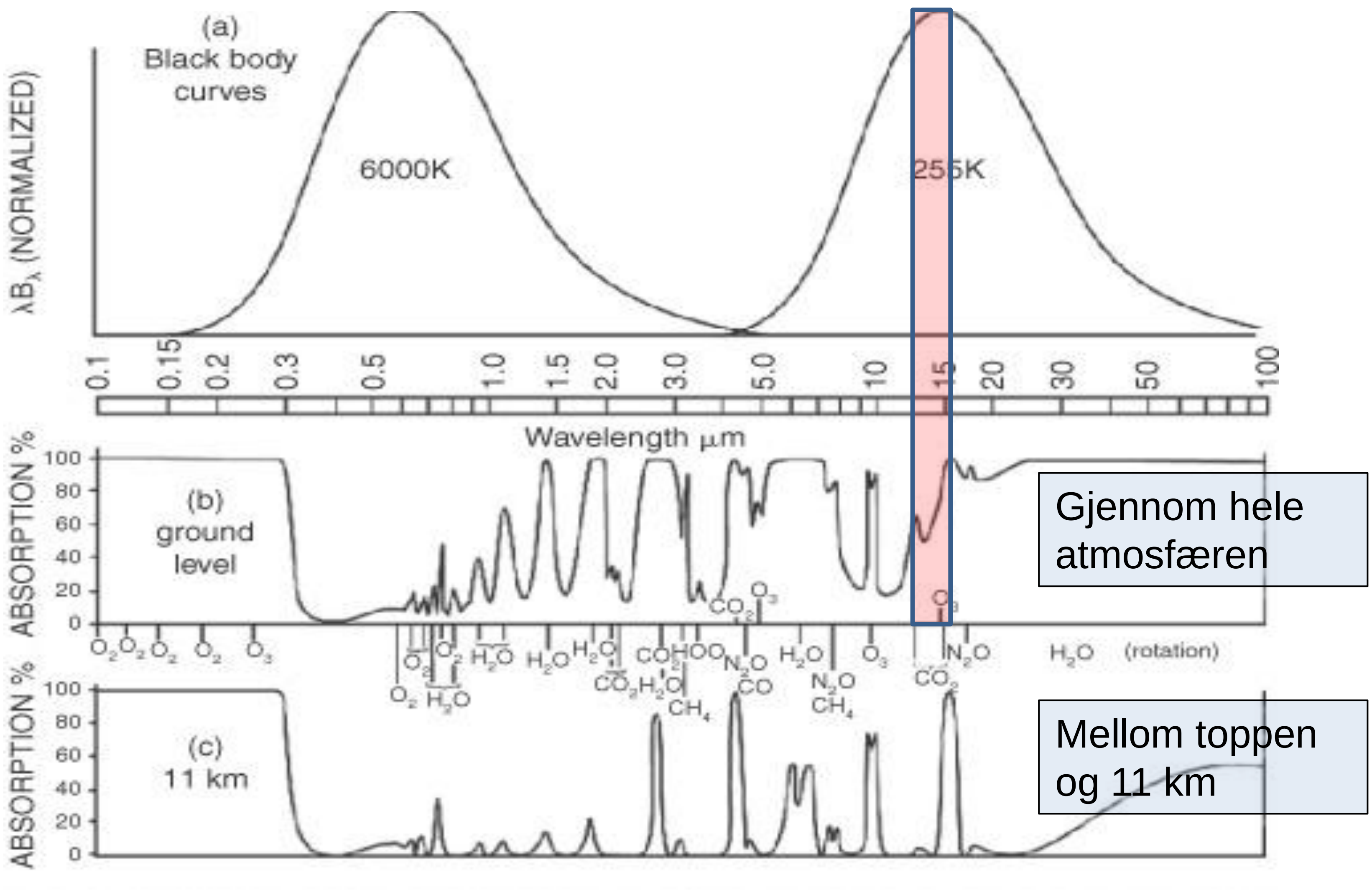
(a)
Black body
curves
λBλ (NORMALIZED)
6000K
255K
0.1
0.15
0.2
0.3
0.5
1.0
1.5
2.0
3.0
5.0
10
15
20
30
50
100
Wavelength μm
(b)
ground
level
ABSORPTION %
(c)
11 km
(rotation)
Gjennom hele atmosfæren
Mellom toppen og 11 km

Strålingspådriv (radiative forcing)

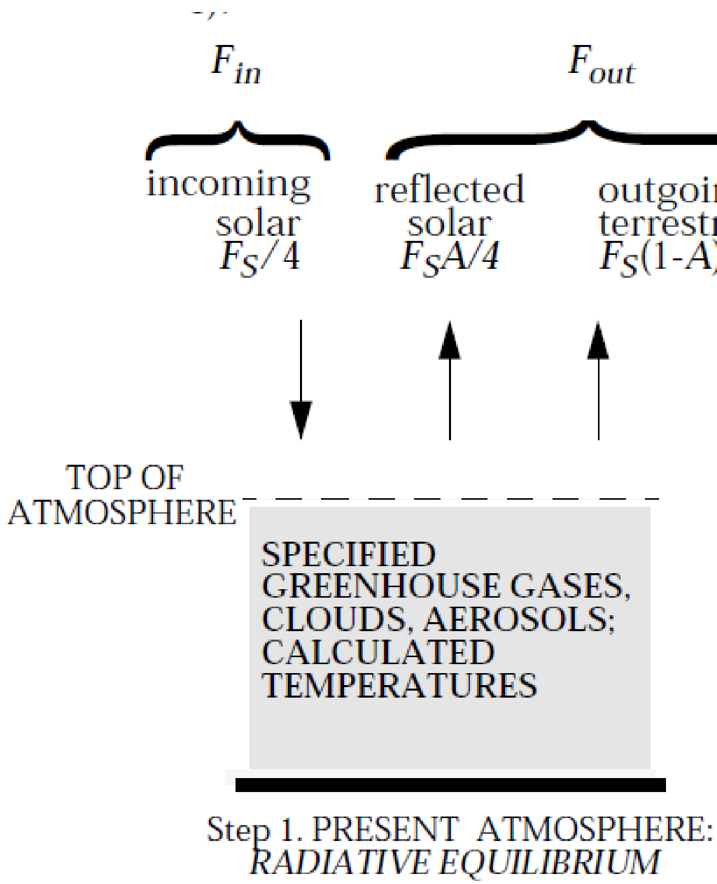

Energiblananse ved stabilt klima:

$F_{in} = F_{out}$

Strålingspådriv (radiative forcing)

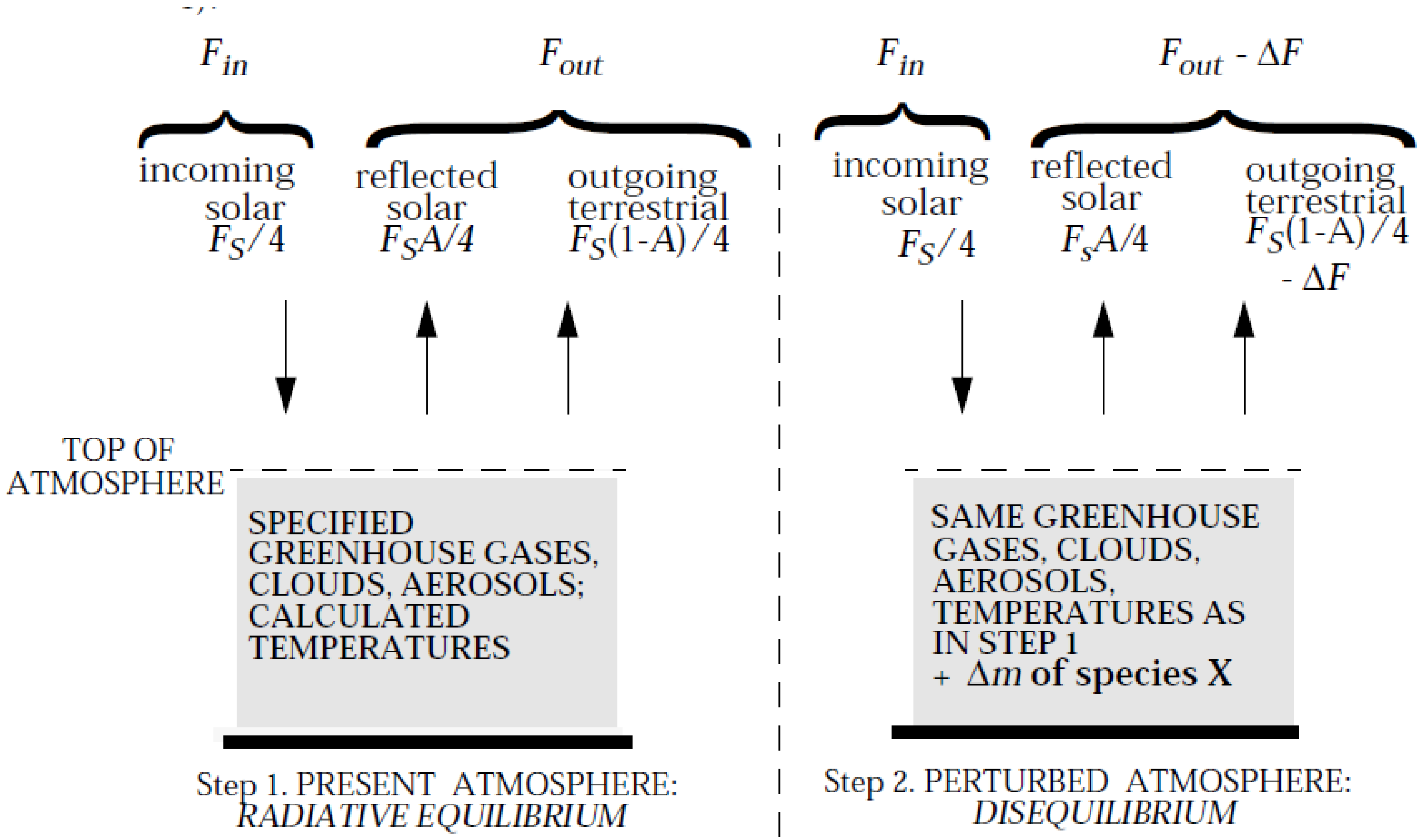

Energibalanse ved stabilt klima:
$F_{in} = F_{out}$

Endret mengde klimagass Δm
➔ Strålingspådriv (ubalanse): ΔF

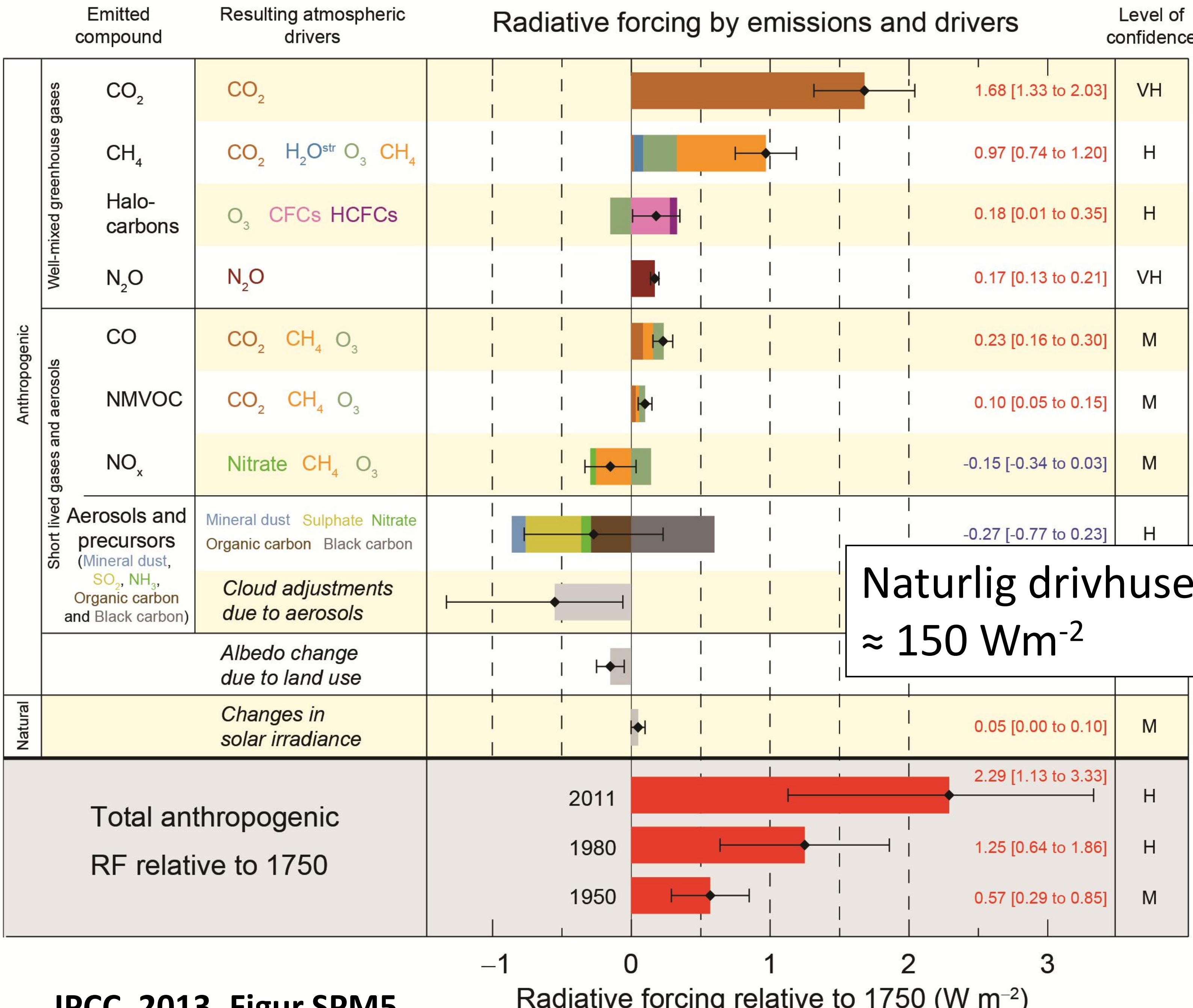

Naturlig drivhuseffekt:

≈ 150 Wm^{-2}

IPCC, 2013. Figur SPM5

Radiative Forcing : Strålingspådriv

NOAA Greenhouse Gas records

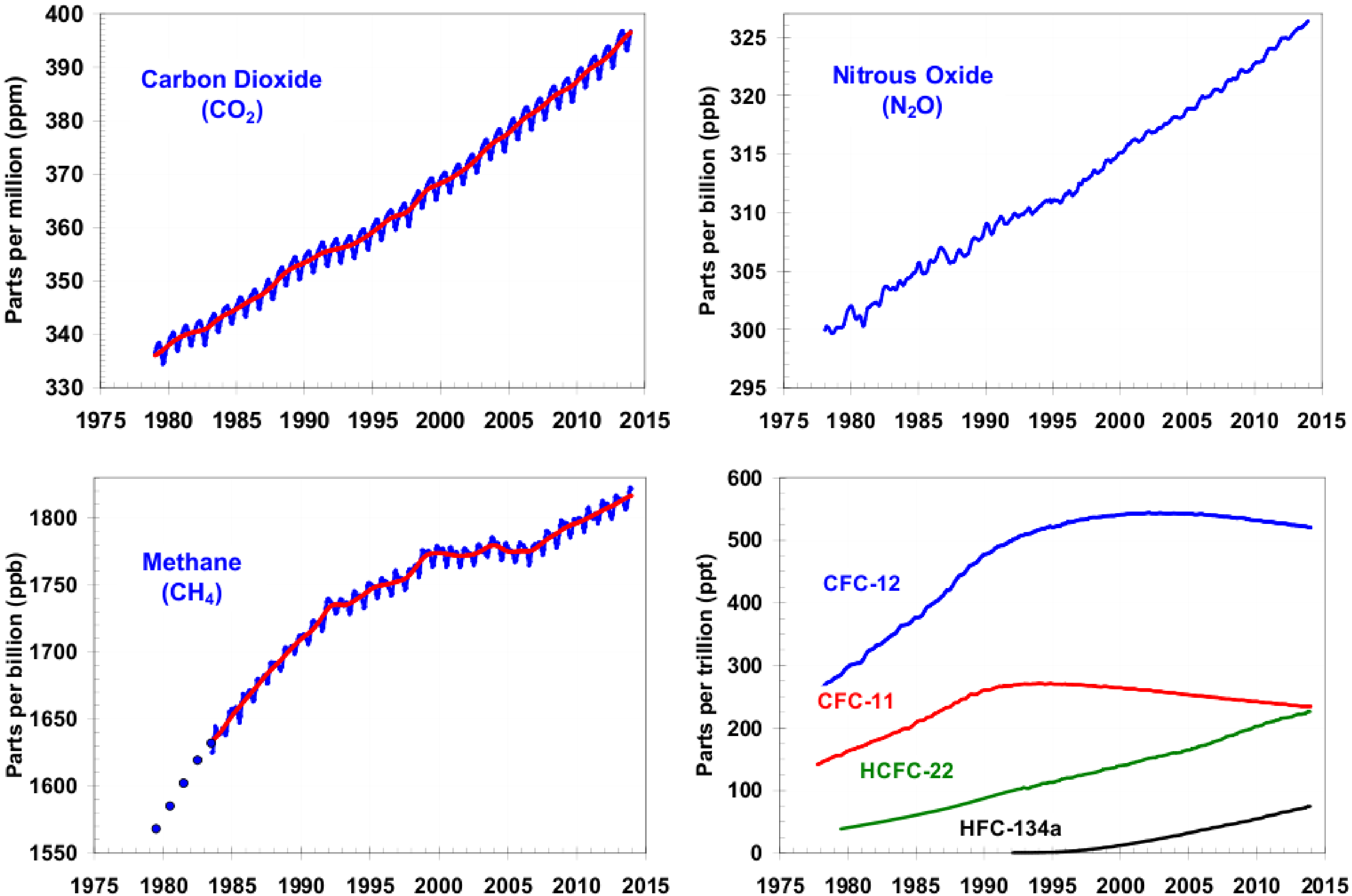

http://www.esrl.noaa.gov/gmd/aggi/

CO_2 konsentrasjoner fra iskjerner (1100 år tilbake)

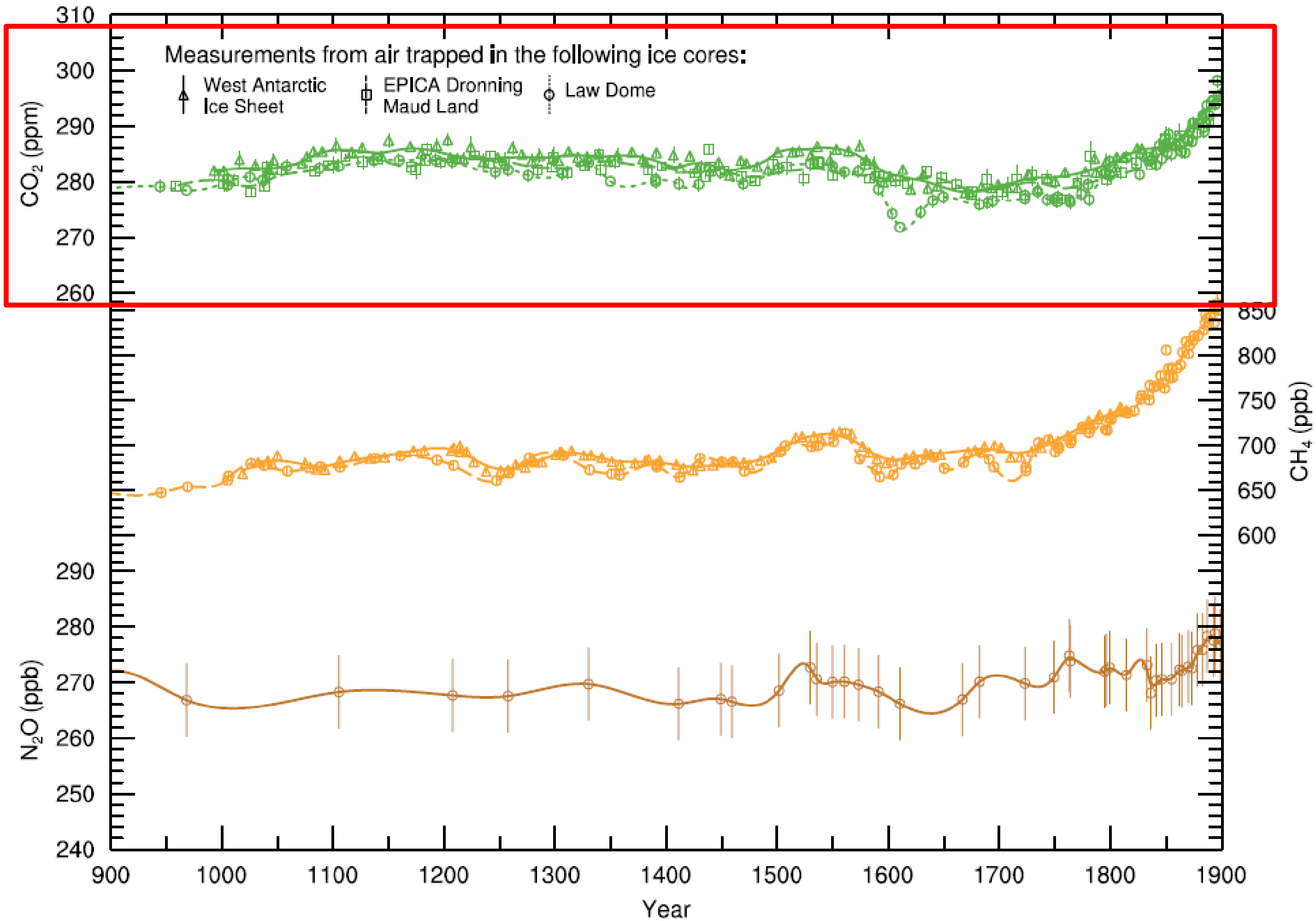

Figure 6.7 | Variations of CO_2, CH_4, and N_2O during 900–1900 from ice cores. The data are for Antarctic ice cores: Law Dome (Etheridge et al., 1996; MacFarling-Meure et al., 2006), circles; West Antarctic Ice Sheet (Mitchell et al., 2011; Ahn et al., 2012), triangles; Dronning Maud Land (Siegenthaler et al., 2005a), squares. Lines are spline fits to individual measurements.

IPCC, 2013

Pådriv og responser i klimasystemet

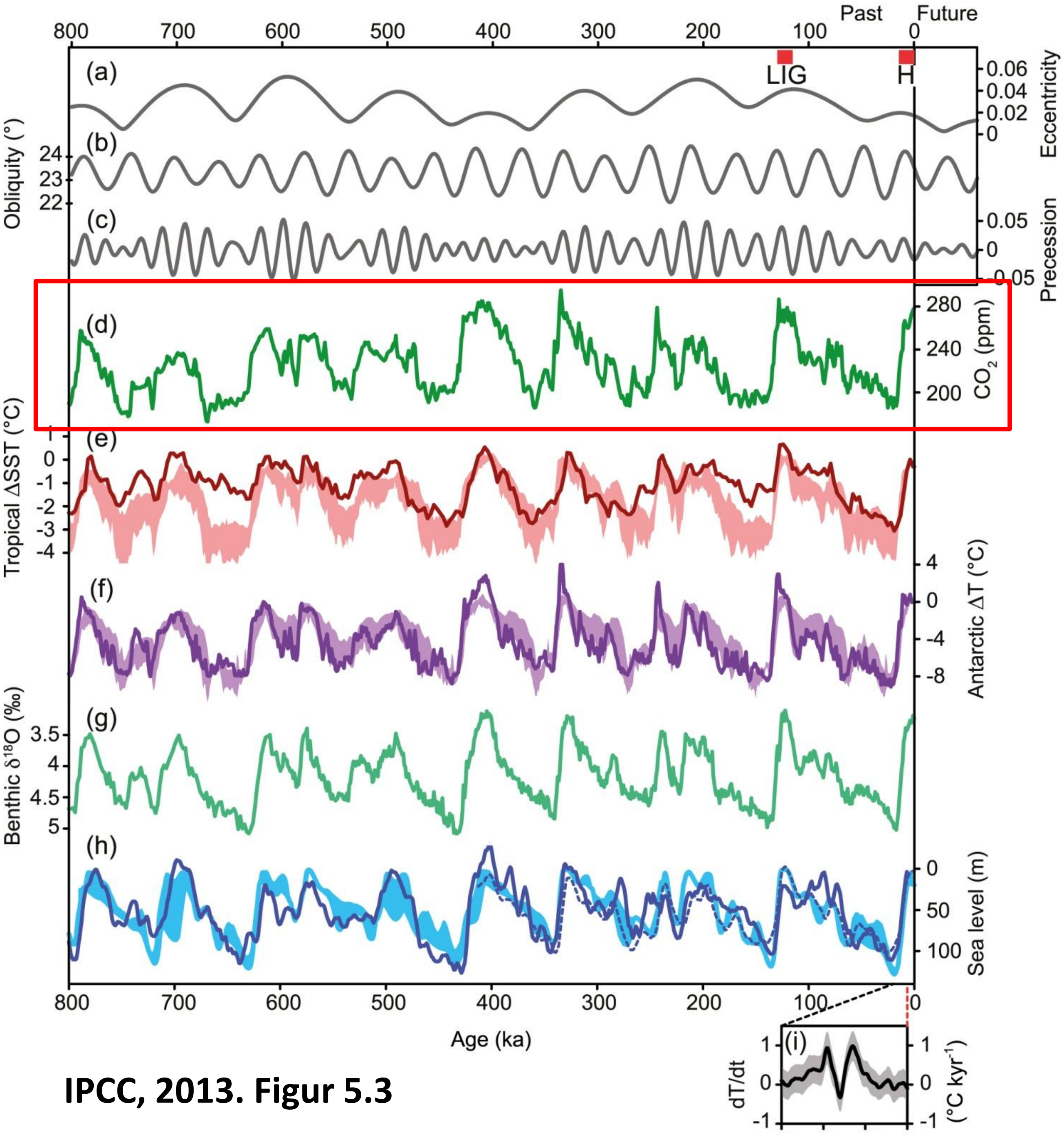

IPCC, 2013. Figur 5.3

Her: Temperaturendringen kommer først

➔CO_2 endringer følger

De siste 150 år: CO_2 økning skyldes hovedsakelig bruk av fossilt brennstoff.

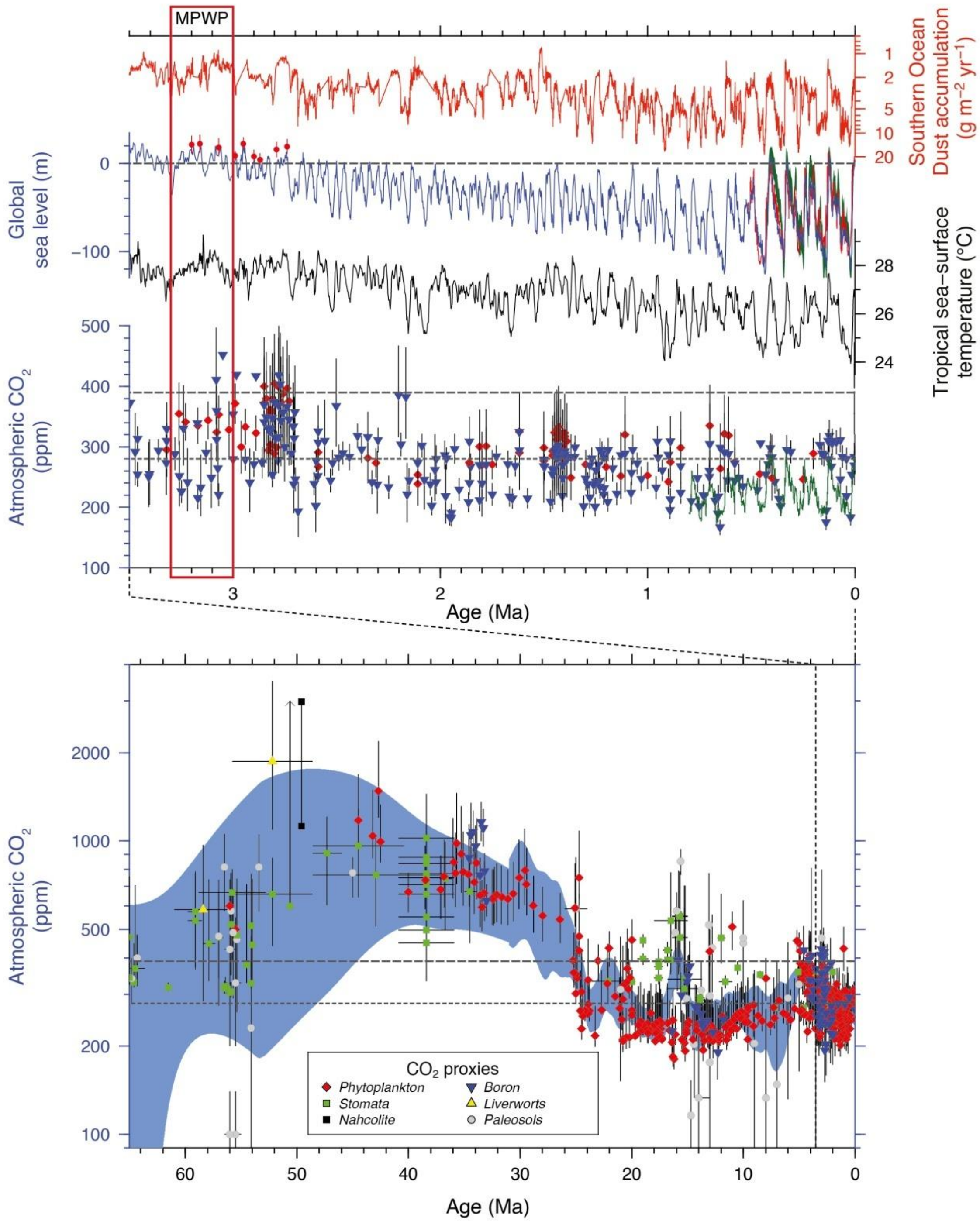

CO_2 konsentrasjoner på geologisk tidsskala (65 mill år)

IPCC, 2013. Figur 5.2

Historiske utslipp (Pg(C)/år)

1 Pg (10^{15} g) = En milliard tonn

1 kg(C) = 3.66 kg(CO_2)

IPCC (2013):
Olje/kull/gass: 9.5 Pg(C)/yr
Avskoging: 1.0 Pg(C)/yr
Økning atm: ≈ 4 Pg(C)/yr
Opptak hav: ≈ 2.5 Pg(C)/yr
➔Opptak land: ≈ 2 Pg(C)/yr

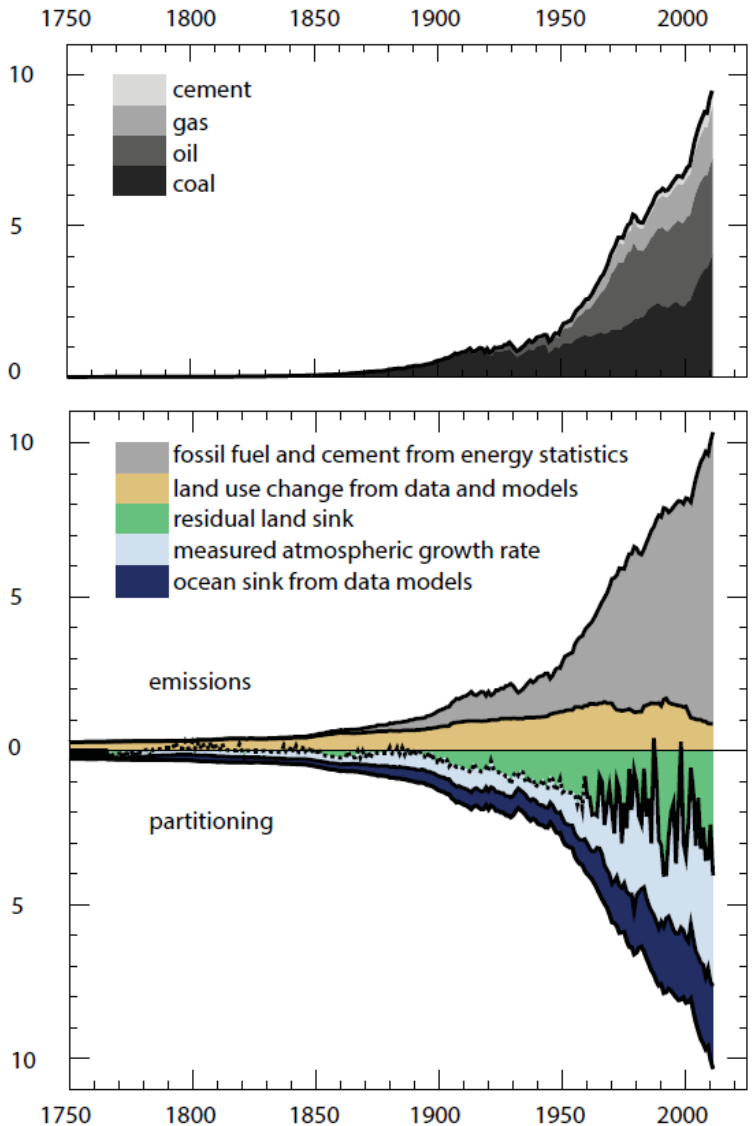

Figure 6.8: Annual anthropogenic CO_2 emissions and their partitioning among the atmosphere, land an[d ocean (PgC] yr^{-1}) from 1750 to 2011. (Top) Fossil fuel and cement CO_2 emissions by category, estimated by the Carbon Dioxide Information Analysis Center (CDIAC) based on UN energy statistics for fossil fuel combustion and US Geological Survey for cement production (Boden et al., 2011). (Bottom) Fossil fuel and cement CO_2 emissions as above. CO_2 emissions from net land use change, mainly deforestation, are based on land cover change data and estimated for 1750–1850 from the average of four models (Pongratz et al., 2009; Shevliakova et al., 2009; van Minnen et al., 2009; Zaehle

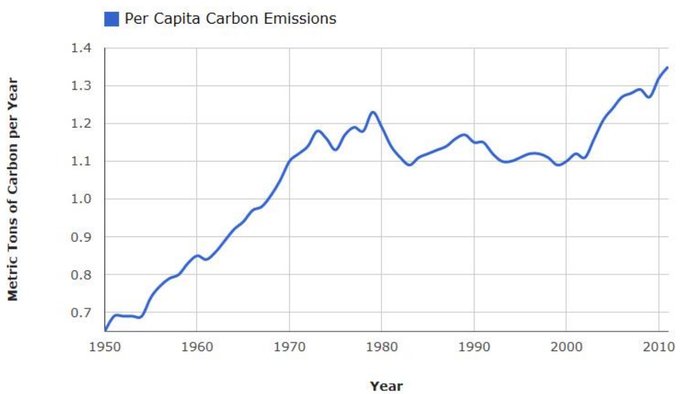

Source: Boden, T.A., G. Marland, and R. J. Andres. 2015. Global, Regional, and National Fossil-Fuel CO_2 Emissions. Carbon Diox[ide] Information Analysis Center, Oak Ridge National Laboratory, U.S. Department of Energy, Oak Ridge, Tenn., U.S.A. doi: 10.3334/CDIAC/00001_V2015.

IPCC, 2013

Det Global karbonbudsjettet

1 Pg = 10^{15} g = 1000 mill tonn

Global Flows of Carbon
(Petagrams of Carbon/Year)

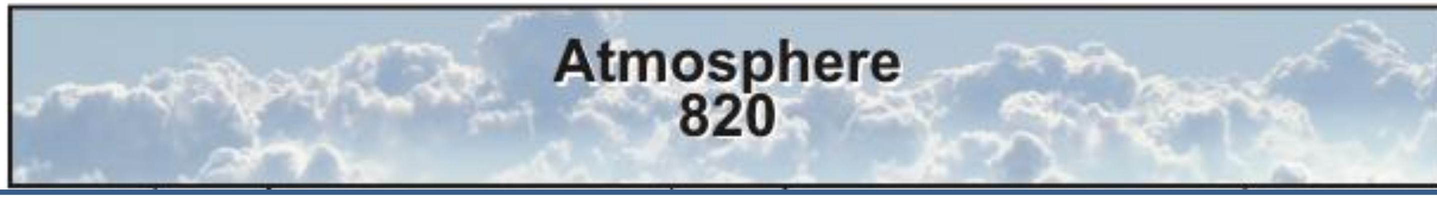

Det Global karbonbudsjettet

1 Pg = 10^{15} g = 1000 mill tonn

Fotosyntese

Respirasjon/

nedbrytning

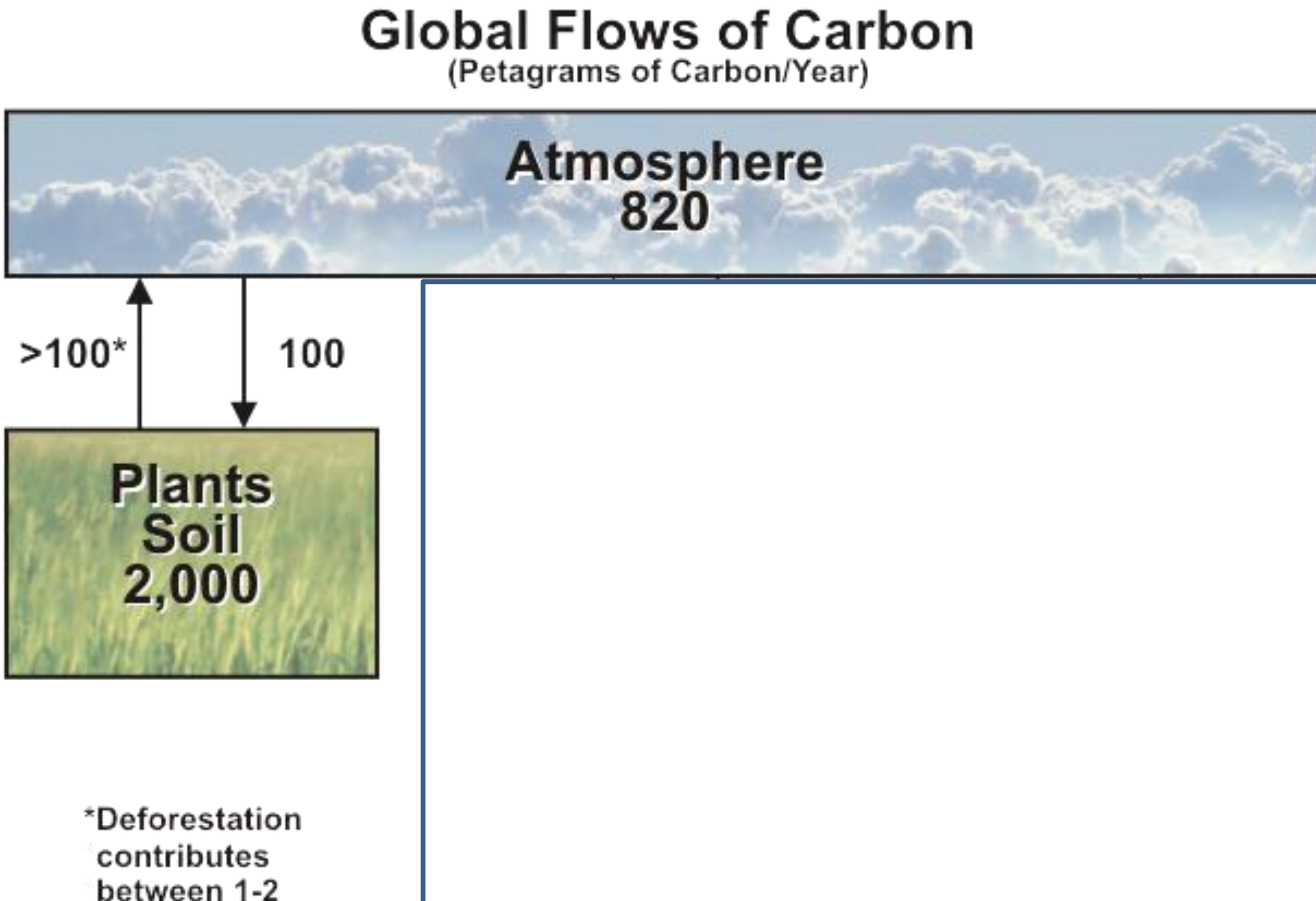

Det Global karbonbudsjettet

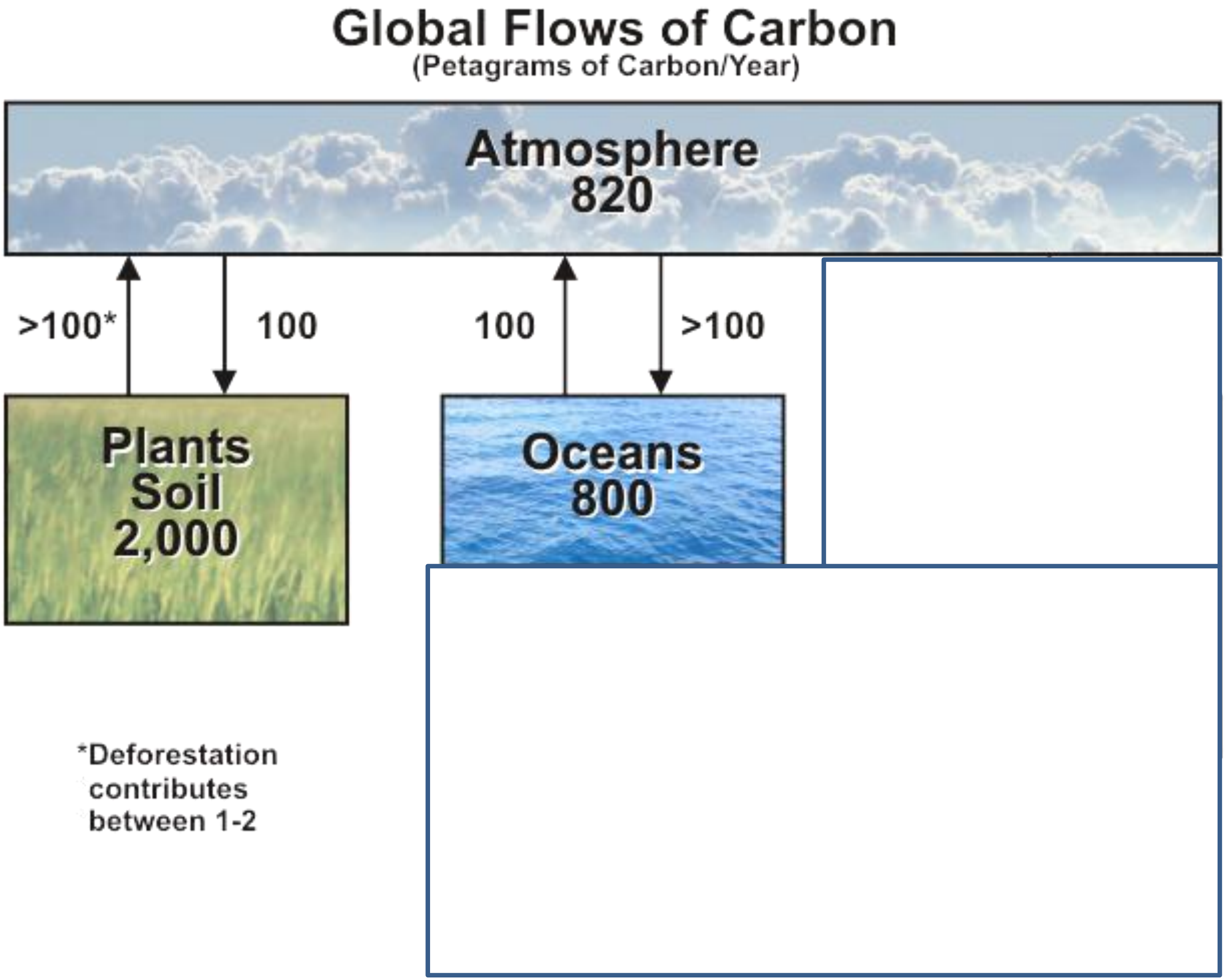

Det Global karbonbudsjettet

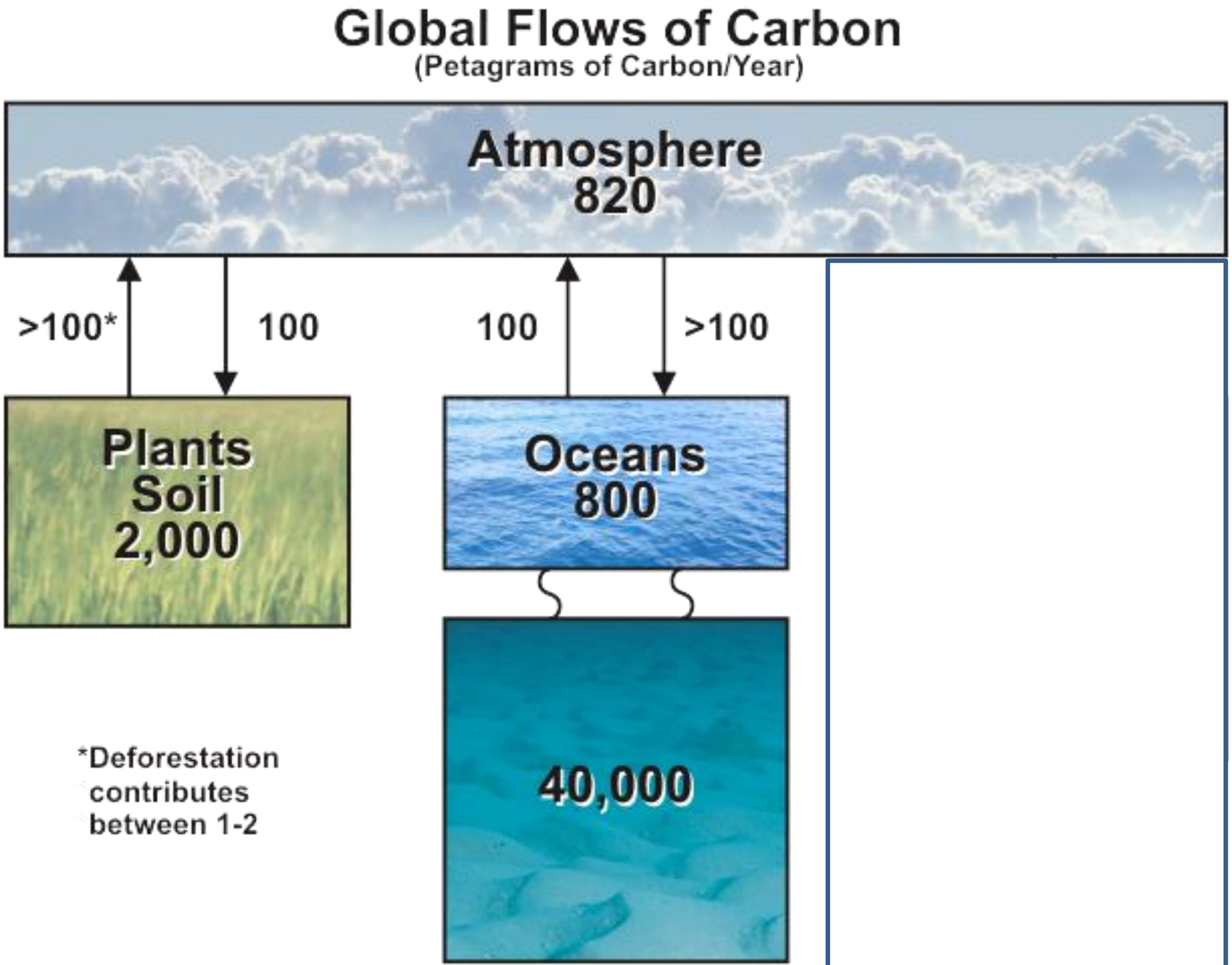

Det Global karbonbudsjettet

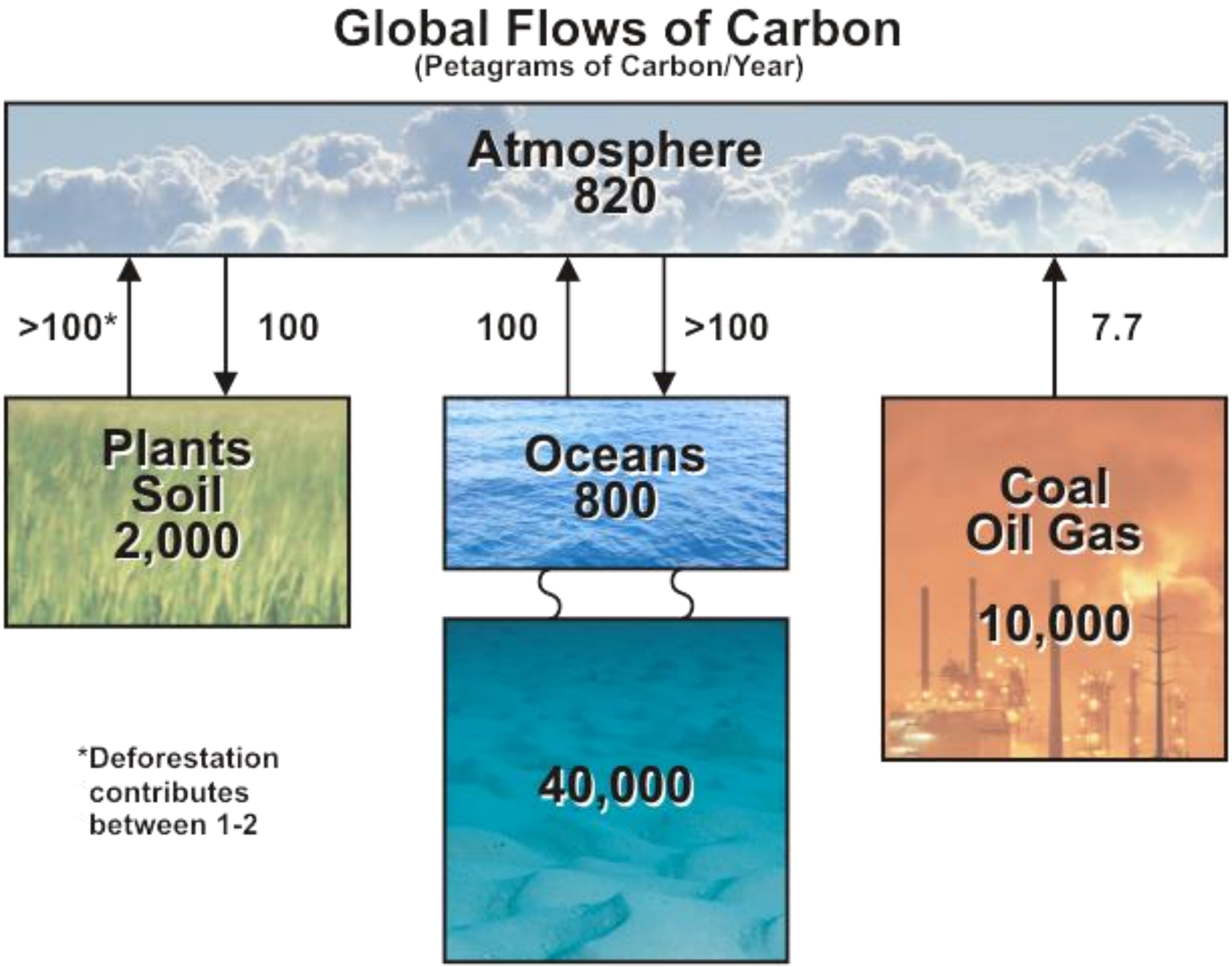

Det Global karbonbudsjettet

- Stor utveksling mellom atmosfære og planter/hav
- Levetid CO_2: 820(PgC)/(100+100 PgC/år) = 4 år
- Mye karbon i dyphavet
- Veldig tregt tap av karbon til olje/kull/gass

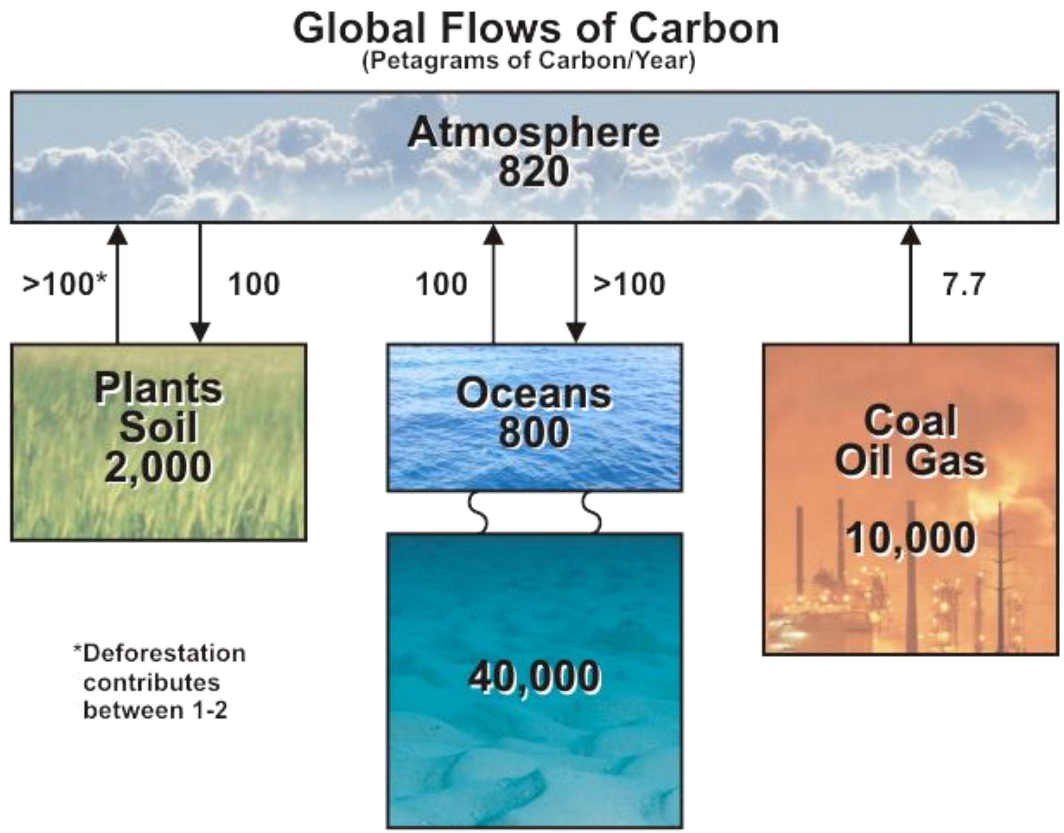

Kilde: https://www.carboncyclescience.us/what-is-carbon-cycle

Det Global karbonbudsjettet

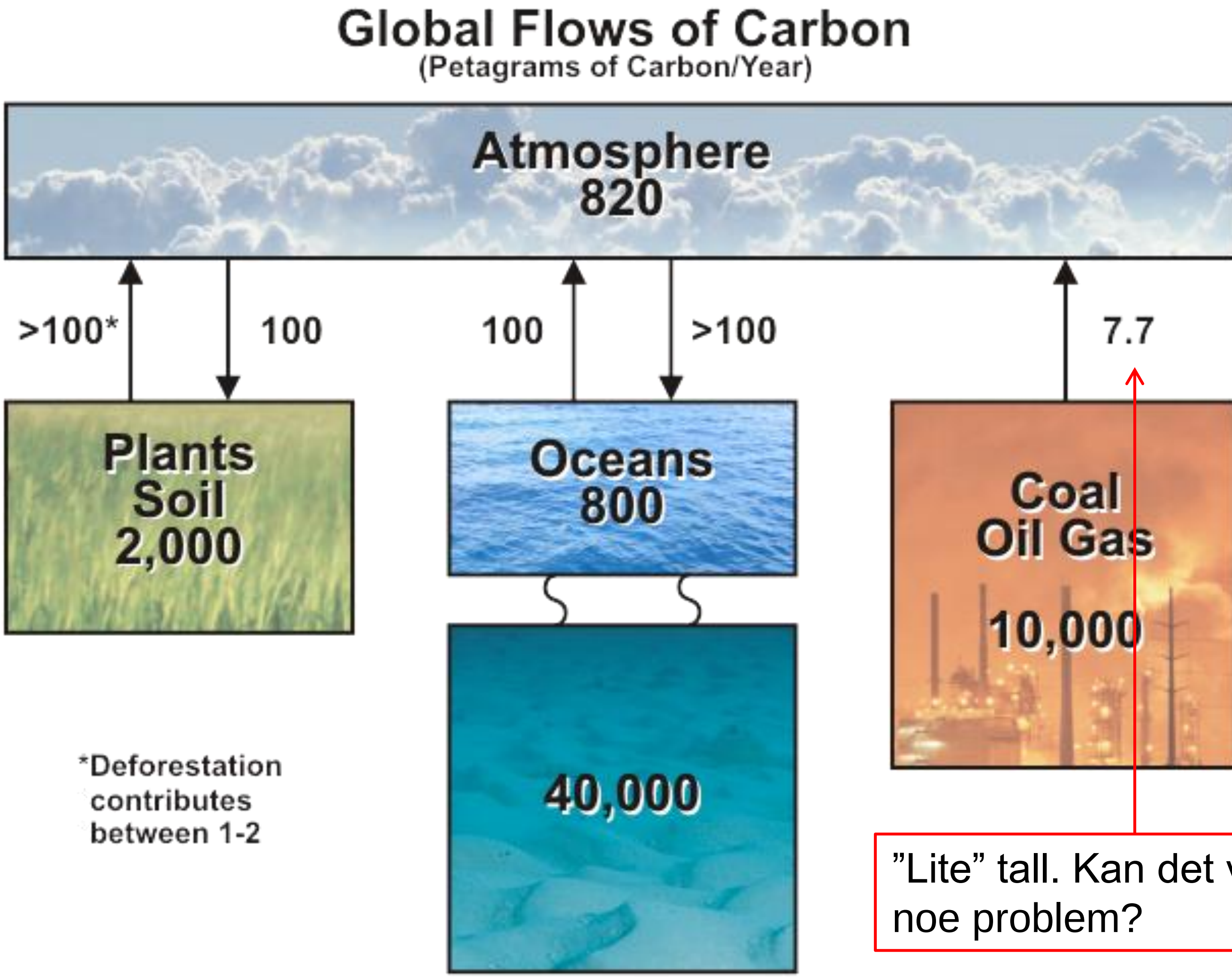

”Lite” tall. Kan det være noe problem?

Forskjell NH/SH skyldes mer utslipp fra fossile kilder i nord.

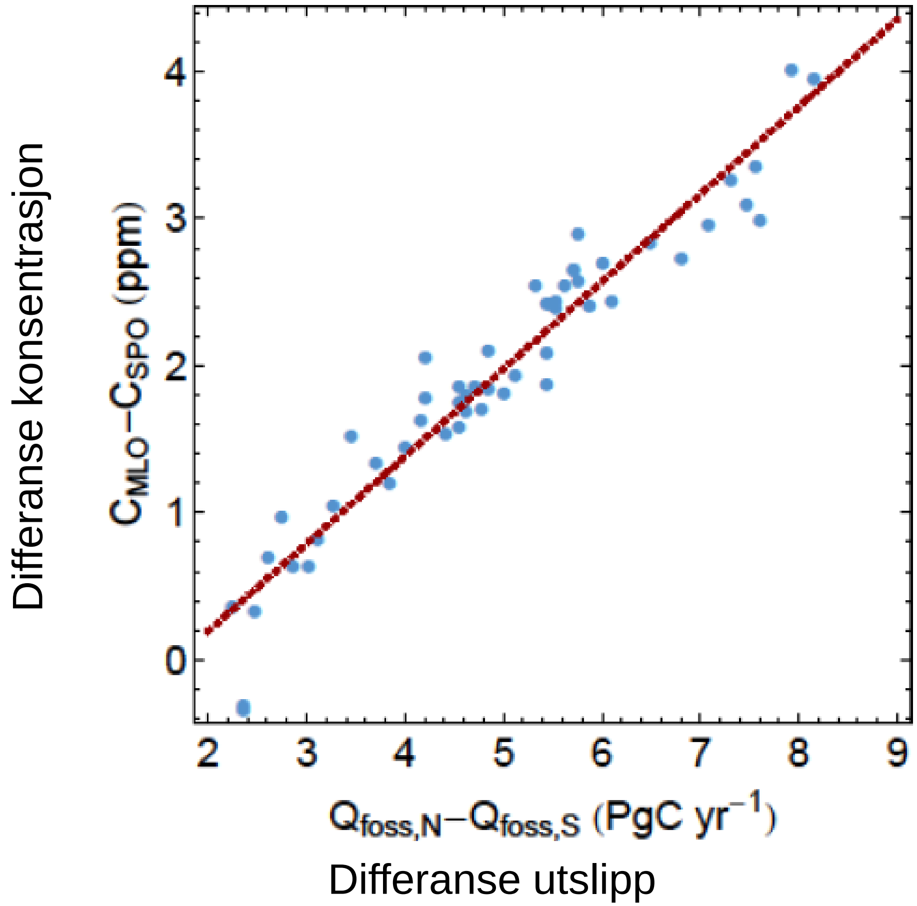

Dersom økningen i CO_2 kom pga. utgassing fra havet ville vi ikke hatt denne forskjellen mellom NH og SH.

Figure 6.13: Blue points: Annually averaged CO_2 concentration difference between the station Mauna Loa in the northern hemisphere and the station South Pole in the southern hemisphere (vertical axis; Keeling et al., 2005, updated) versus the difference in fossil fuel combustion CO_2 emissions between the hemispheres (Boden et al., 2011). Dark red dashed line: regression line fitted to the data points.

IPCC, 2013

CO_2 går opp, mens O_2 går tilsvarende ned
➔ Forbrenning viktig kilde

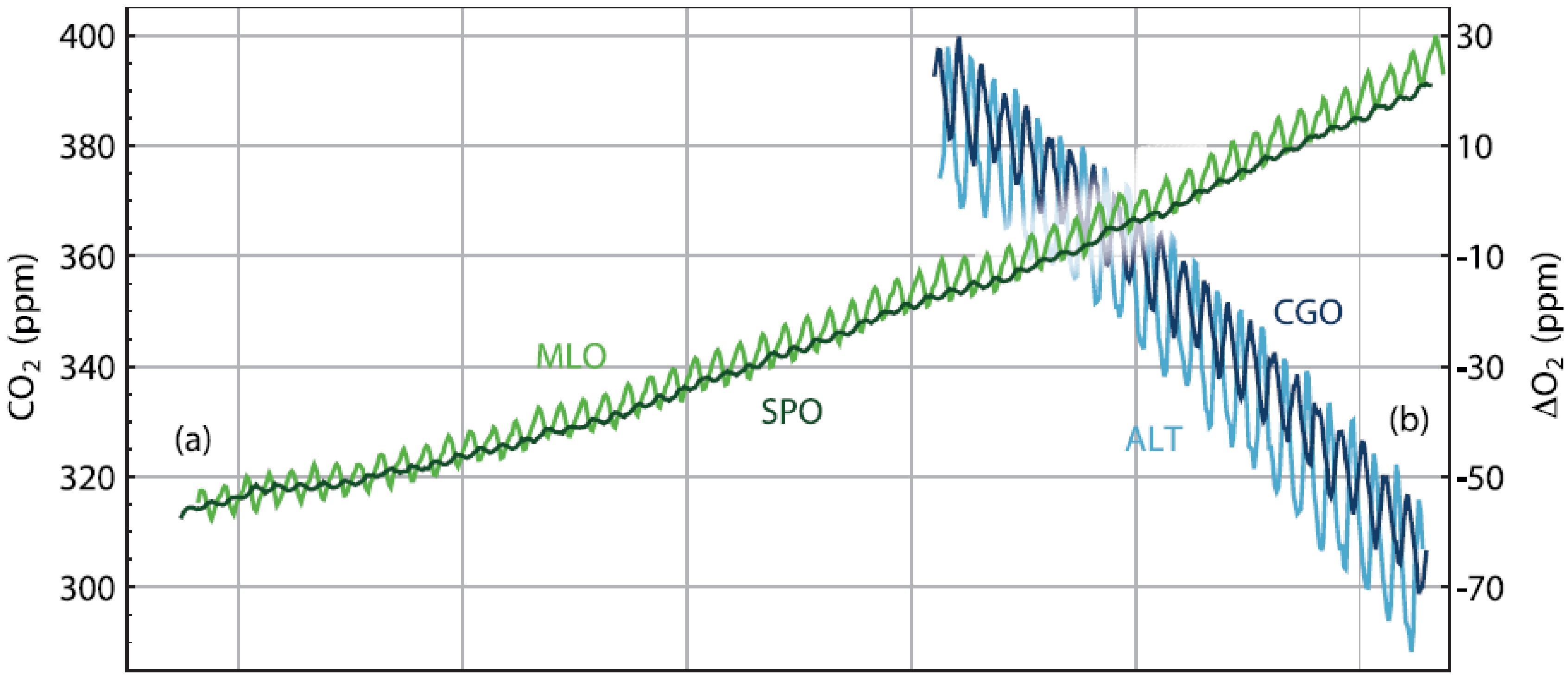

IPCC, 2013

Det globale karbonbudsjettet

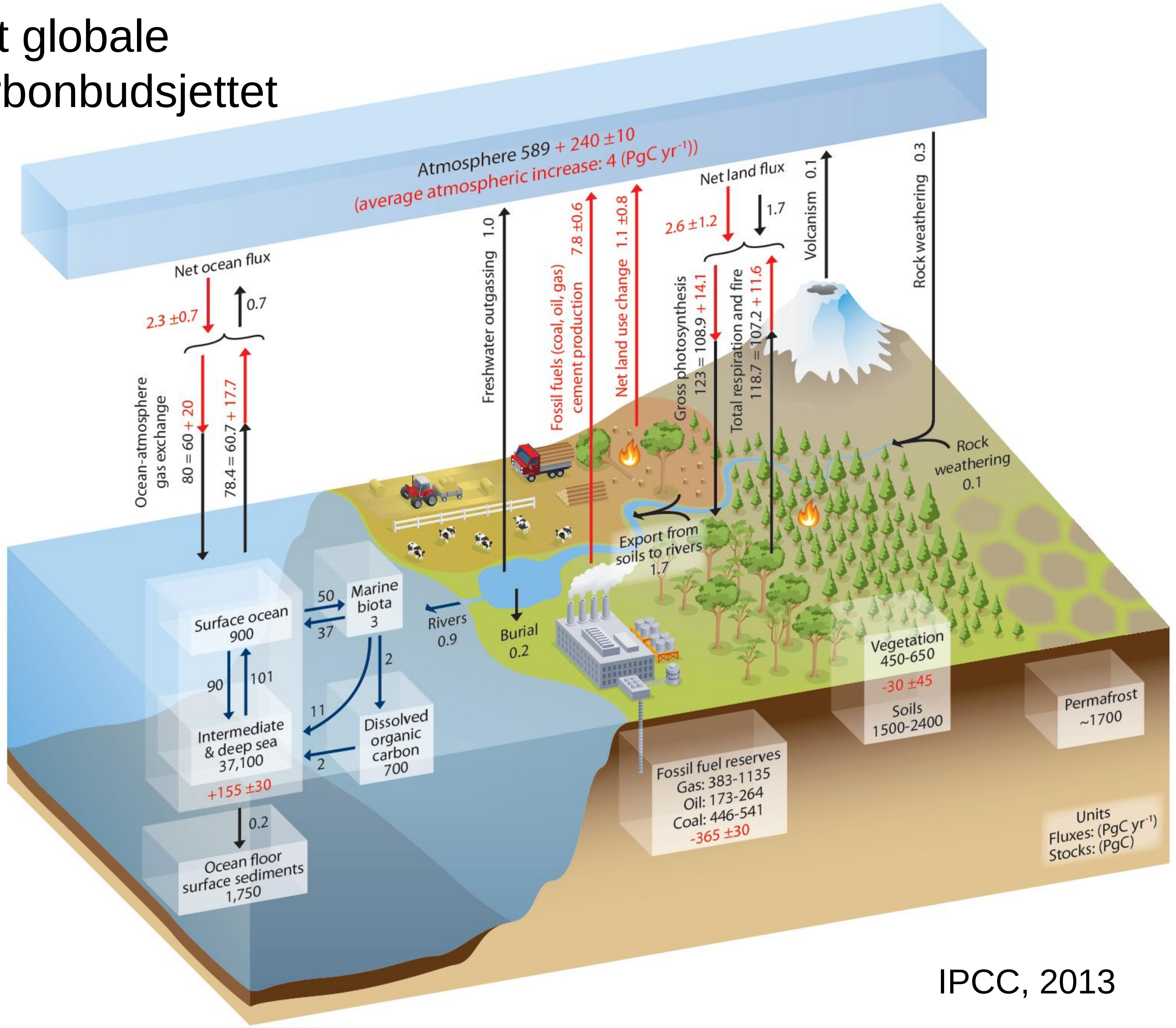

IPCC, 2013

Hvor raskt fjernes CO_2 fra atmosfæren?

- **Levetid (τ)**: Gjennomsnittlig oppholdstid for et CO_2 molekyl i atmosfæren
  τ= Masse i atm./opptak(hav+bakke)≈820/(100+100)≈4 år

- **Justeringstid** (adjustment time): Tid det tar for å fjerne et ekstra utslipp til atmosfæren.
  - Naturlige kretsløp var i balanse
  - ➔ Mye lengre enn levetiden fordi opptakene er lite avhengige av konsentrasjonen i atmosfæren

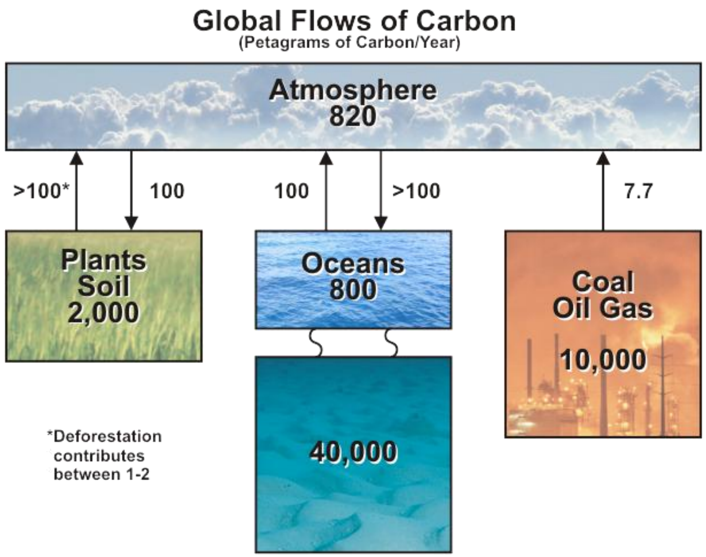

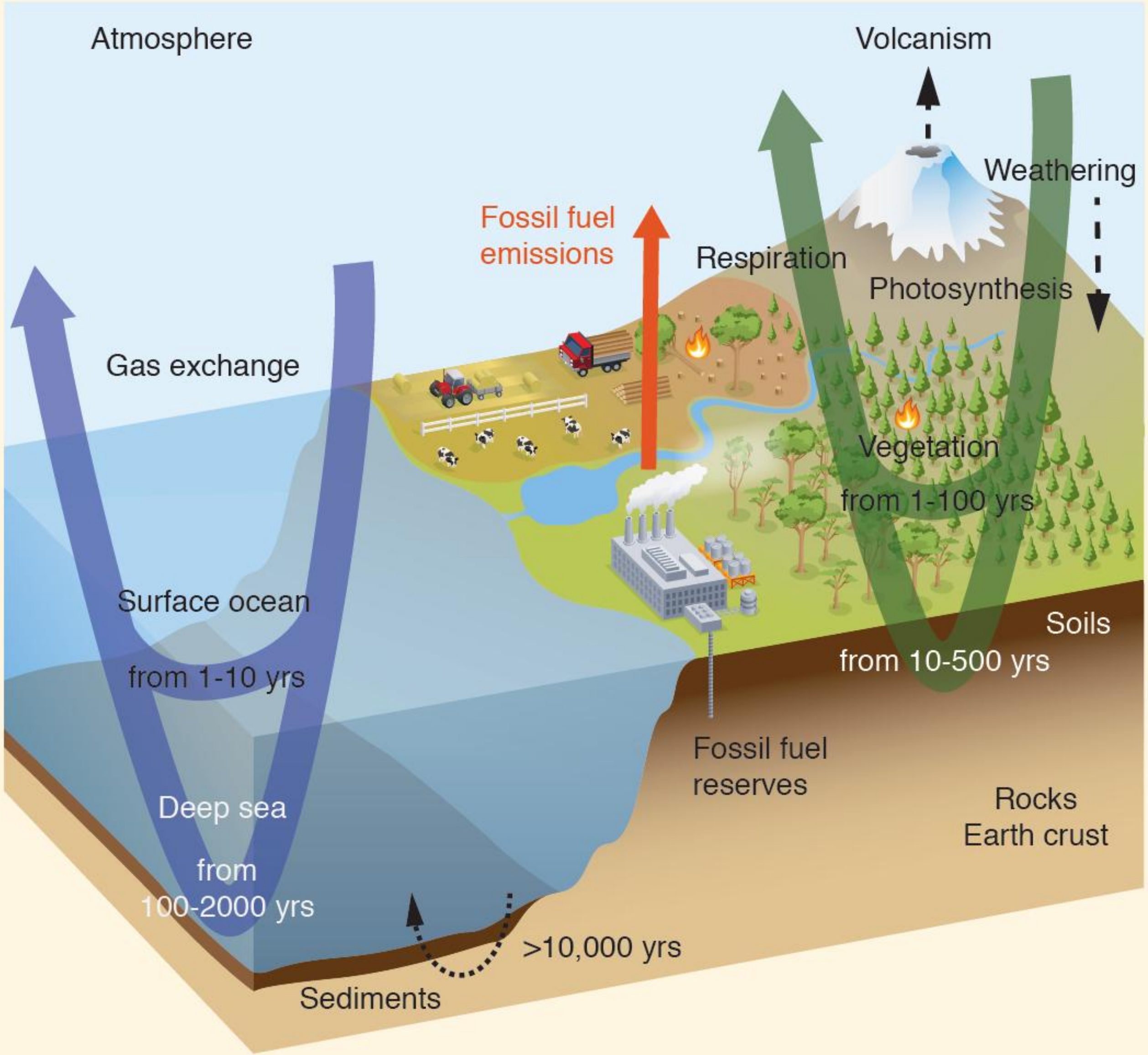

FAQ 6.2, Figure 1 | Simplified schematic of the global carbon cycle showing the typical turnover time scales for carbon transfers through the major reservoirs.

Tidsskalaer for utveksling av karbon mellom reservoarene

IPCC, 2013

Karbonkjemi i havet

M=mol/liter (Molar)

- CO_2 løses i vannet og danner $CO_2 \cdot H_2O$
  - Likevekt ved Henrys lov
    $K_H = [CO_2 \cdot H_2O]/P_{CO2} = 3 \cdot 10^{-2}$ M/atm
- $CO_2 \cdot H_2O$ dissosierer og danner HCO_3^- og H^+
  - $K_1 = [HCO_3^-][H^+]/[CO_2 \cdot H_2O] = 9 \cdot 10^{-7}$ M
- HCO_3^- dissosierer og danner CO_3^{2-} og H^+
  - $K_2 = [CO_3^{2-}][H^+]/[HCO_3^-] = 7 \cdot 10^{-10}$ M

$$CO_2(g) \overset{H_2O}{\Leftrightarrow} CO_2 \cdot H_2O \qquad \text{(R3)}$$

$$CO_2 \cdot H_2O \Leftrightarrow HCO_3^- + H^+ \qquad \text{(R4)}$$

$$HCO_3^- \Leftrightarrow CO_3^{2-} + H^+ \qquad \text{(R5)}$$

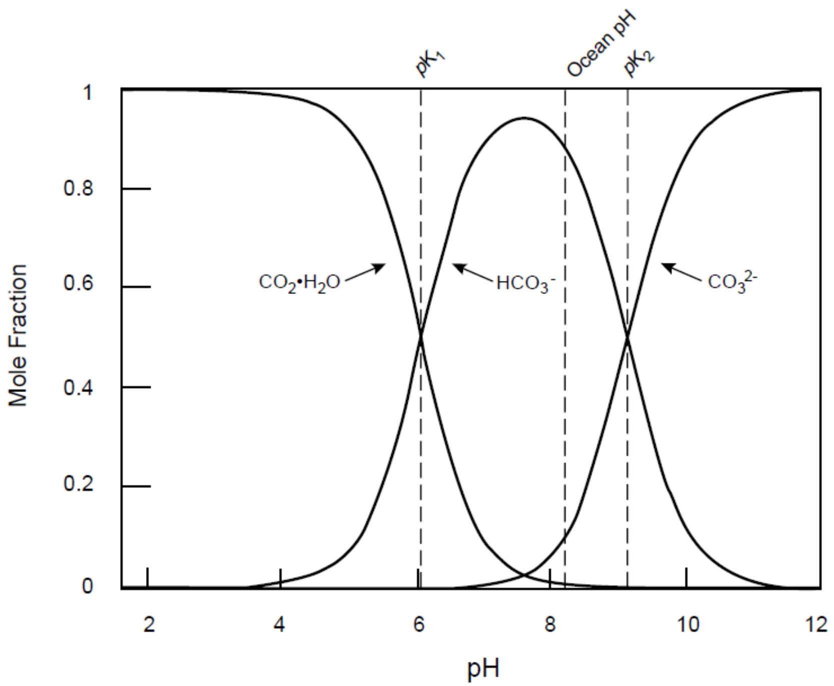

Figure 6-7 Speciation of total carbonate CO_2(aq) in seawater vs. pH

pH = -log [H^+]

Lav pH ➔ [H^+] høy

[H^+] høy ➔ R5 og R4 forskjøvet mot venstre

pH i havet (pre-industrielt): 8.2

Buffereffekten av HCO_3^- og CO_3^{2-}

$$CO_2(g) \overset{H_2O}{\Leftrightarrow} CO_2 \cdot H_2O \qquad \text{(R3)}$$

$$CO_2 \cdot H_2O \Leftrightarrow HCO_3^- + H^+ \qquad \text{(R4)}$$

$$HCO_3^- \Leftrightarrow CO_3^{2-} + H^+ \qquad \text{(R5)}$$

$$CO_2(g) + CO_3^{2-} \overset{H_2O}{\Leftrightarrow} 2HCO_3^- \qquad \text{(R6)}$$

NB! Buffereffekten hindrer ikke at [H⁺] øker, men demper økningen betydelig

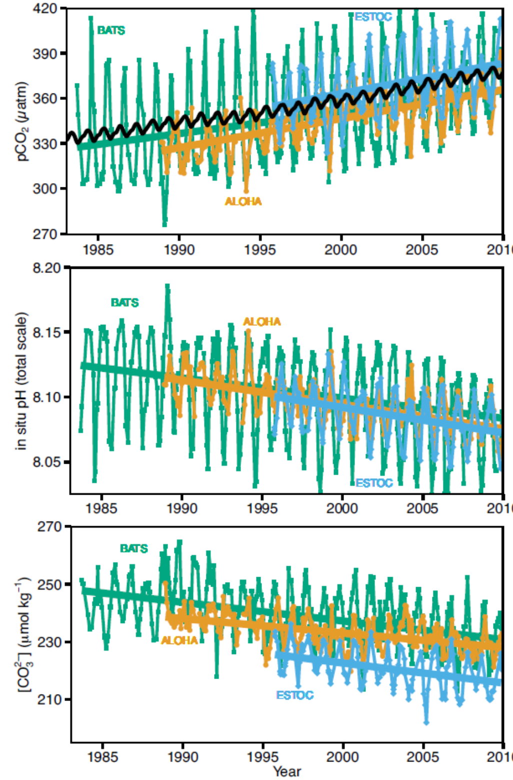

Figure 3.18: Long-term trends of surface seawater pCO_2 (top), pH (middle), and carbonate ion (bottom) concentration at three subtropical ocean time series in the North Atlantic and North Pacific Oceans, including: **a)** Bermuda Atlantic Time-series Study (BATS, 31°40′N, 64°10′W; **green**) and Hydrostation S (32°10′, 64°30′W) from 1983 to present (updated from Bates, 2007); **b)** Hawaii Ocean Time-series (HOT) at Station ALOHA (A Long-term Oligotrophic Habitat Assessment; 22°45′N, 158°00′W; **orange**) from 1988 to present (updated from Dore et al., 2009), and; **c)** European Station for Time series in the Ocean (ESTOC, 29°10′N, 15°30′W; **blue**) from 1994 to present (updated from González-Dávila et al., 2010). Atmospheric pCO_2 (**black**) from the Mauna Loa Observatory Hawaii is shown in the top panel. Lines show linear fits to the data, whereas Table 3.2 give results for harmonic fits to the data (updated from Orr, 2011).

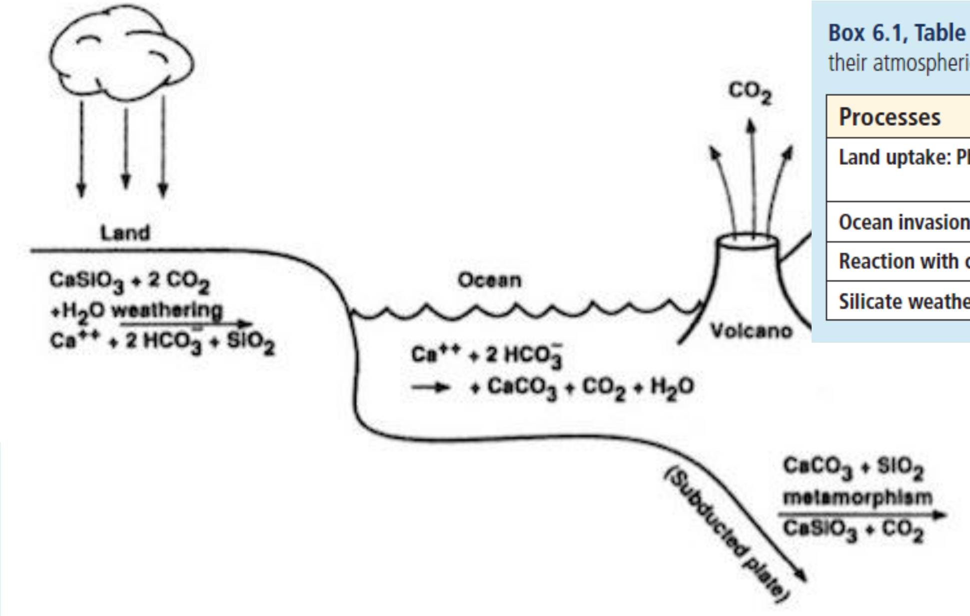

Box 6.1, Table 1 | The main natural processes that remove CO_2 consecutive to a large emission pulse to the atmosphere, their atmospheric CO_2 adjustment time scales, and main (bio)chemical reactions involved.

Processes	Time scale (years)	Reactions
Land uptake: Photosynthesis–respiration	$1–10^2$	$6CO_2 + 6H_2O$ + photons $\rightarrow C_6H_{12}O_6 + 6O_2$ $C_6H_{12}O_6 + 6O_2 \rightarrow 6CO_2 + 6H_2O$ + heat
Ocean invasion: Seawater buffer	$10–10^3$	$CO_2 + CO_3^{2-} + H_2O \rightleftharpoons 2HCO_3^-$
Reaction with calcium carbonate	$10^3–10^4$	$CO_2 + CaCO_3 + H_2O \rightarrow Ca^{2+} + 2HCO_3^-$
Silicate weathering	$10^4–10^6$	$CO_2 + CaSiO_3 \rightarrow CaCO_3 + SiO_2$

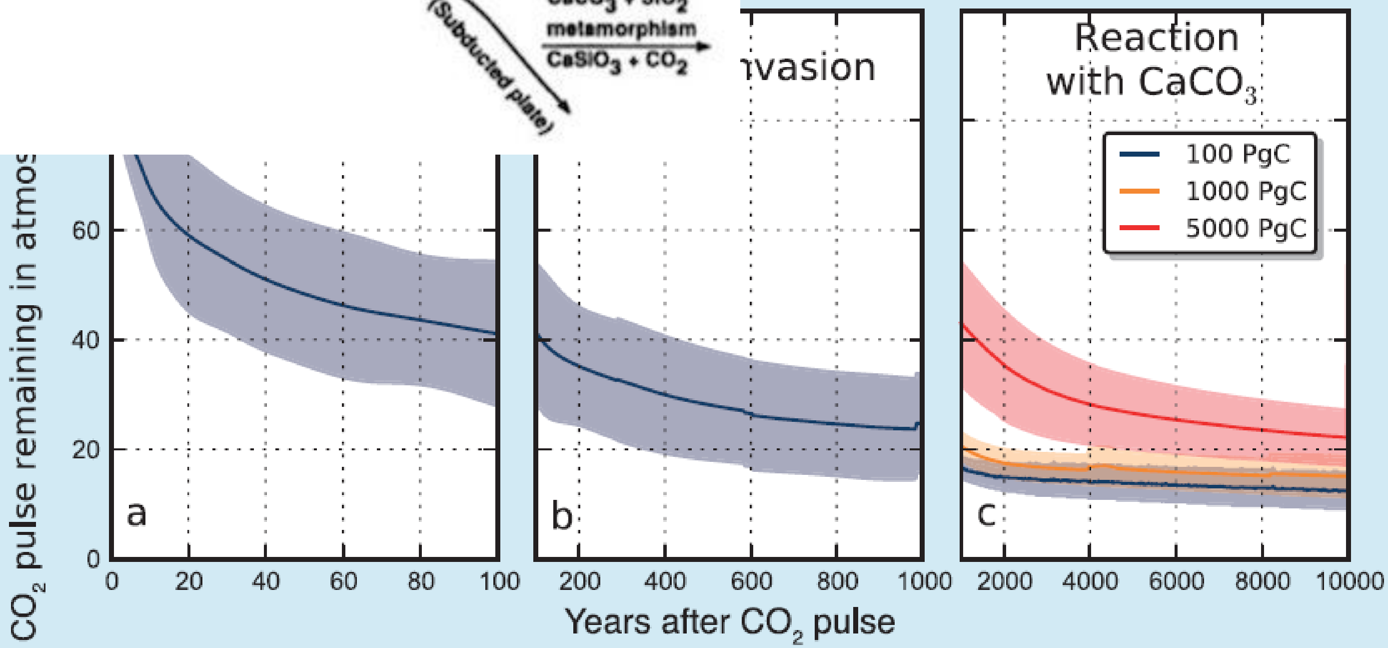

Box 6.1, Figure 1 | A percentage of emitted CO_2 remaining in the atmosphere in response to an idealised instantaneous CO_2 pulse emitted to the atmosphere in year 0 as calculated by a range of coupled climate–carbon cycle models. (Left and middle panels, a and b) Multi-model mean (blue line) and the uncertainty interval (±2 standard deviations, shading) simulated during 1000 years following the instantaneous pulse of 100 PgC (Joos et al., 2013). (Right panel, c) A mean of models with oceanic and terrestrial carbon components and a maximum range of these models (shading) for instantaneous CO_2 pulse in year 0 of 100 PgC (blue), 1000 PgC (orange) and 5000 PgC (red line) on a time interval up to 10 kyr (Archer et al., 2009b). Text at the top of the panels indicates the dominant processes that remove the excess of CO_2 emitted in the atmosphere on the successive time scales. Note that higher pulse of CO_2 emissions leads to higher remaining CO_2 fraction (Section 6.3.2.4) due to reduced carbonate buffer capacity of the ocean and positive climate–carbon cycle feedback (Section 6.3.2.6.6).

CO_2 opptak i havet ➔ forsuring av havet

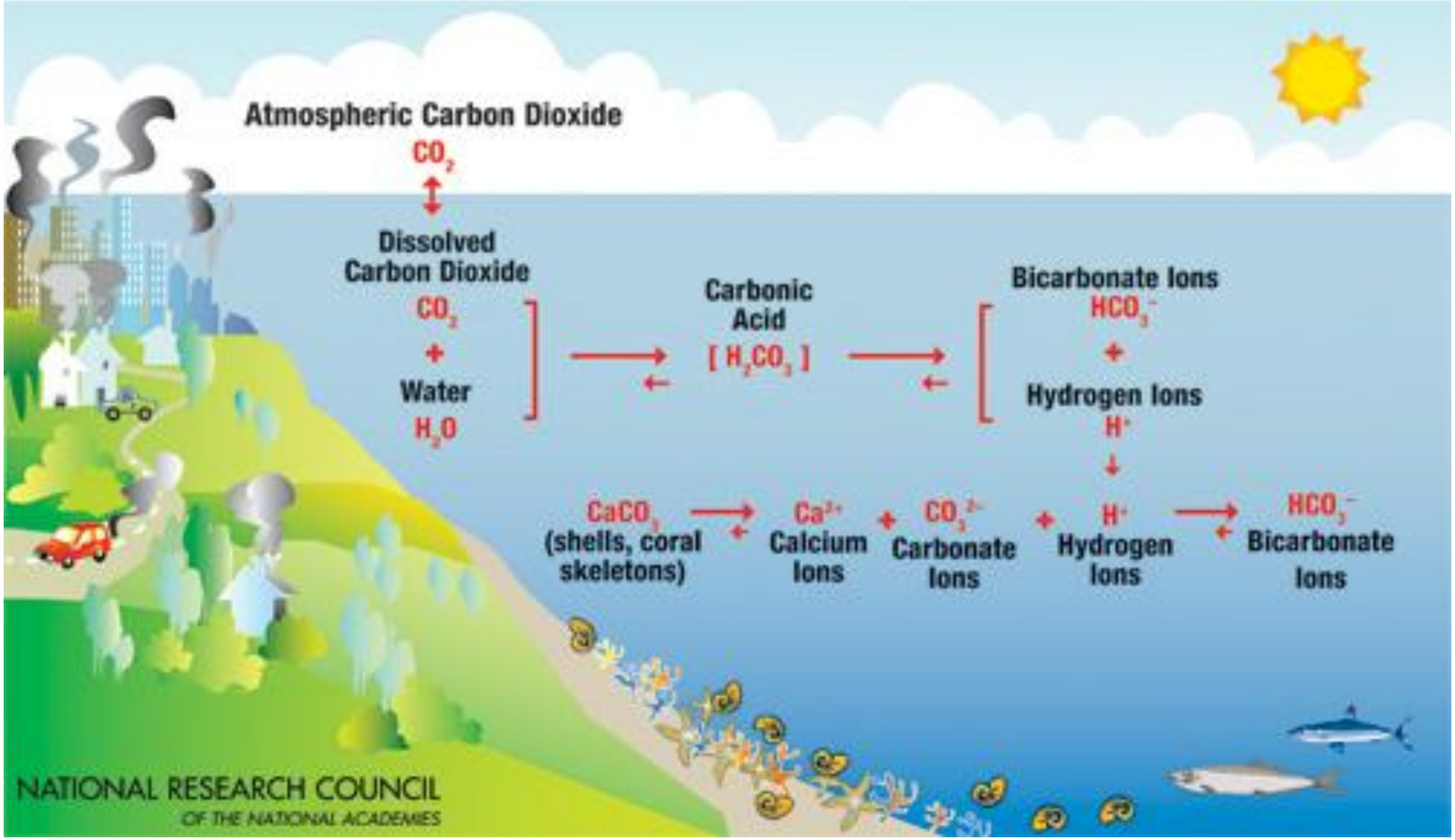

http://oceanacidification.msi.ucsb.edu/people/uta-passow

CO_2 opptak i havet til nå (mol m^{-2})

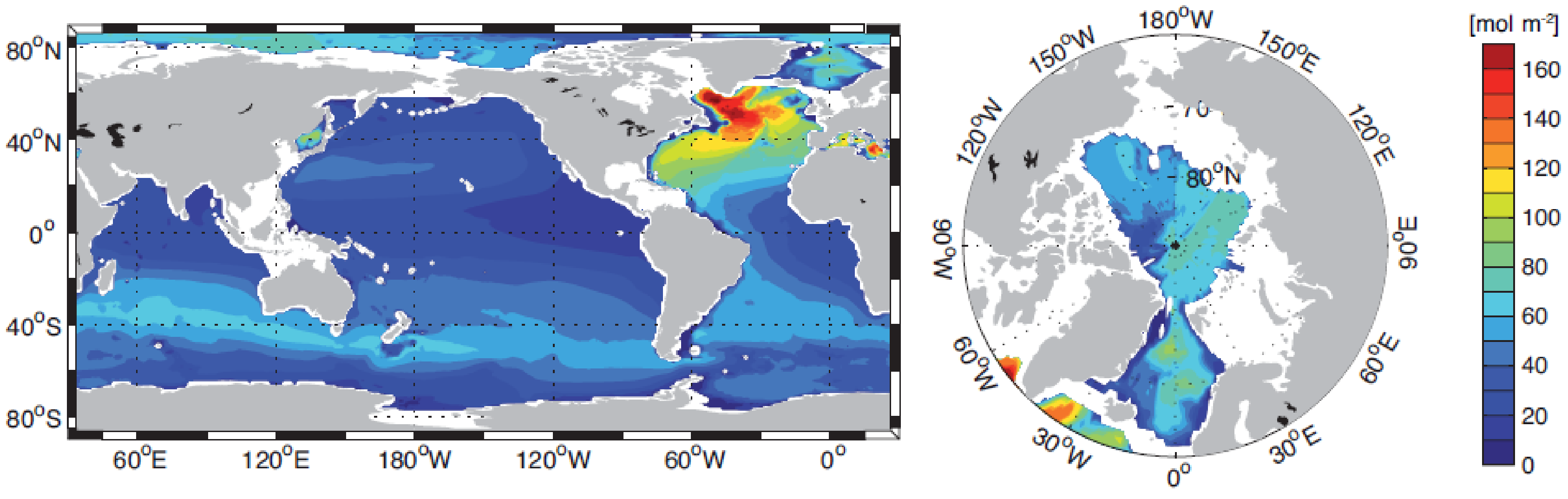

Figure 3.16: Compilation of the 2010 column inventories (mol m^{-2}) of anthropogenic CO_2: the global Ocean excluding the marginal seas (updated from Khatiwala et al., 2009) 150 ± 26 PgC; Arctic Ocean (Tanhua et al., 2009) 2.7–3.5 PgC; the Nordic Seas (Olsen et al., 2010) 1.0–1.6 PgC; the Mediterranean Sea (Schneider et al., 2010) 1.6–2.5 PgC; the East Sea (Sea of Japan) (Park et al., 2006) 0.40 ± 0.06 PgC. From Khatiwala et al. (2013).

IPCC, 2013

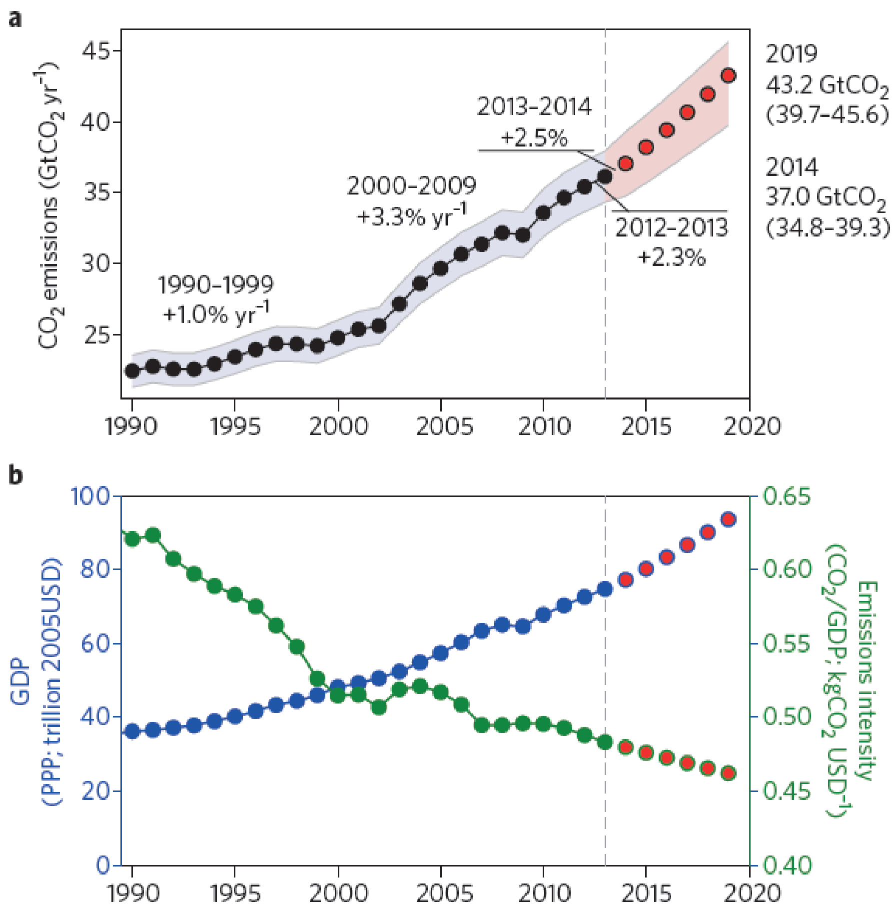

Figure 1 | Global CO_2 emissions and decomposition into GDP and carbon intensity. a,**b**, Global CO_2 emissions from fossil fuel combustion and cement production (**a**; black dots); and global GDP (blue dots) and carbon intensity of GDP (I_{FF}, green dots) (**b**) over 1990–2013 period and estimates to 2019 (red dots). Historical emissions are from CDIAC and BP, while GDP are from IEA and IMF (Methods). Uncertainty in CO_2 emissions is ± 5% (1σ) over the historical period with an additional uncertainty for the projection based on a sensitivity analysis of GDP and I_{FF}. PPP, purchasing power parity.

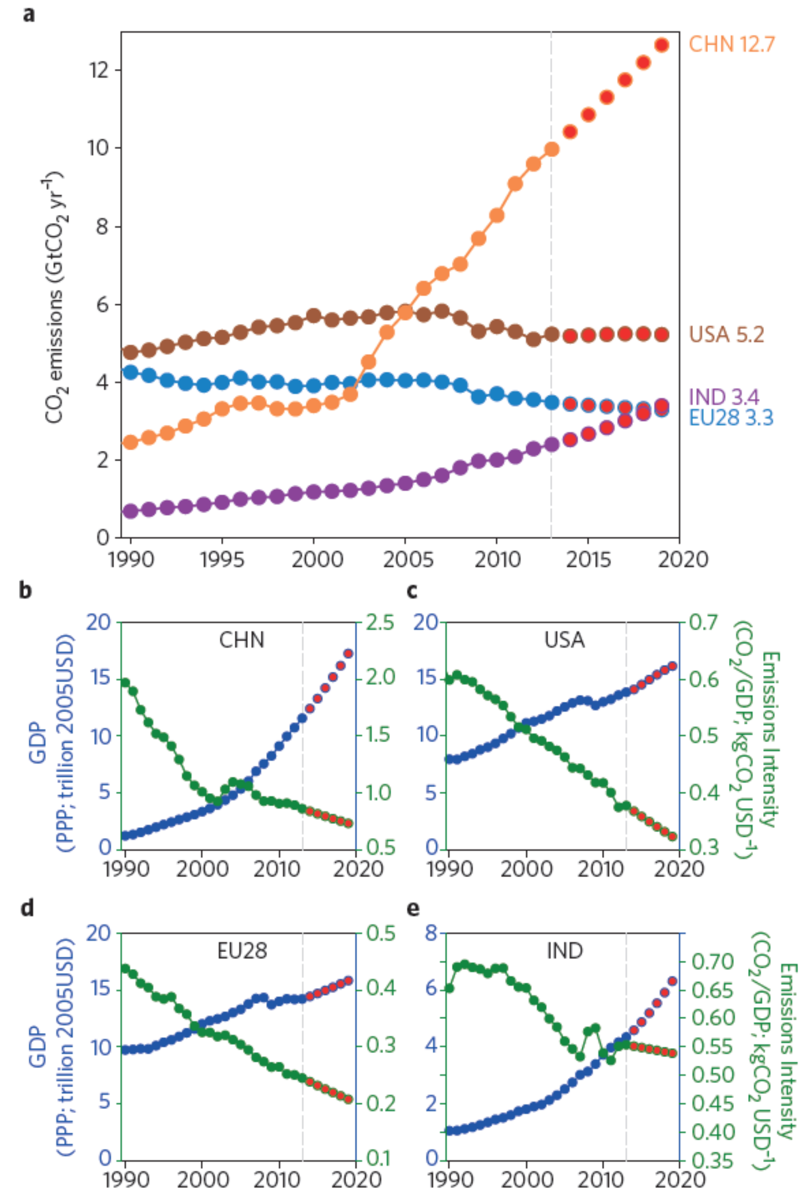

Figure 2 | Regional CO_2 emissions and decomposition into GDP and carbon intensity. a,**b**, The CO_2 emissions from the top four emitters (China, US, EU28, India) (**a**) and the GDP and I_{FF} in each region (**b**–**e**) over the historical (1990–2013) and future (2014-2019) periods. See Fig. 1 caption for details and Supplementary Fig. 2 for an annual decomposition of the trends.

Biogeokjemiske tilbakekoblinger

- Temperaturen øker ➔ økt/redusert plantevekst ➔ økt/red CO_2 opptak ➔ negativ/positiv tilbakekobling
- CO_2 øker ➔ økt plantevekst ➔ økt CO_2 opptak ➔ negative tlibakekobling (såkalt non-climate feedback)
  - Økt tilførsel av nitrogen (bl.a. fra kunstgjødsel og forbrenning) øker CO_2 opptaket

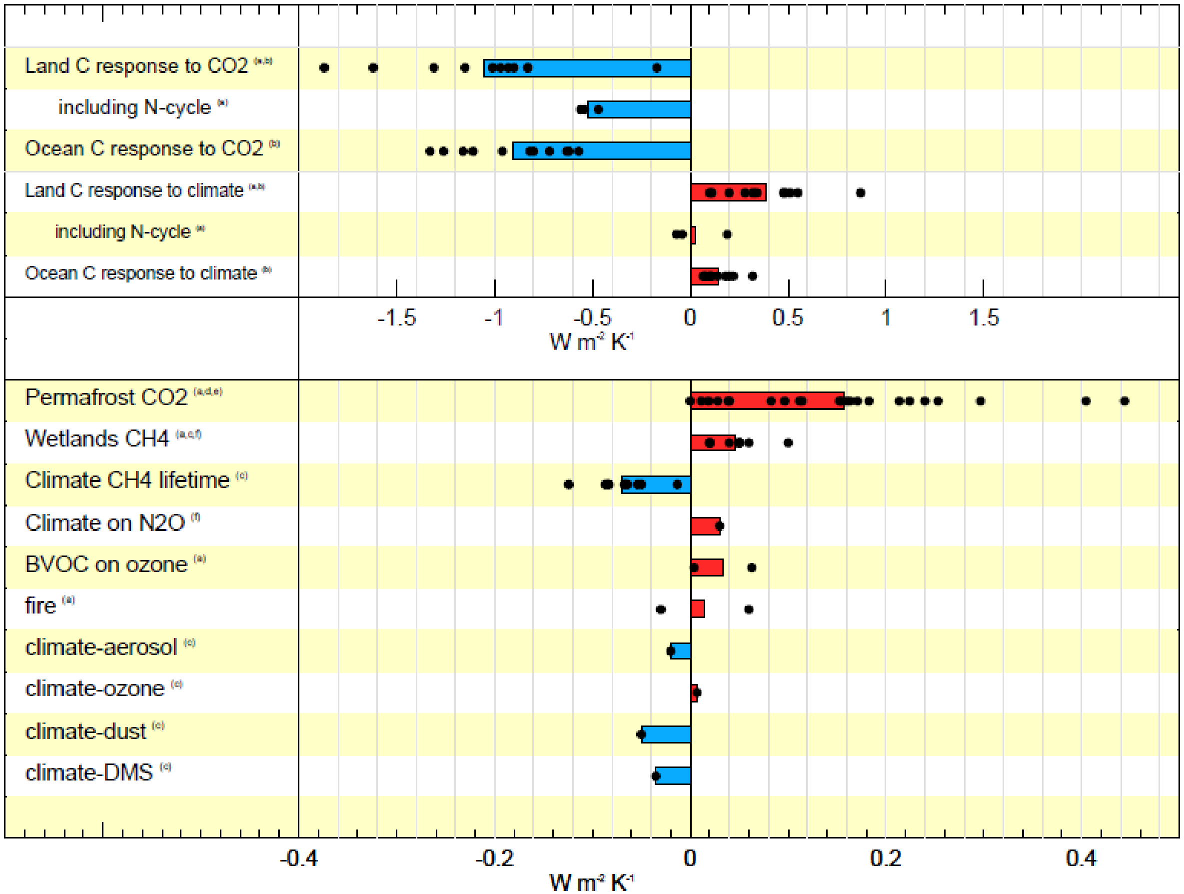

Biogeokjemiske tilbakekoblinger i klimasystemet.

IPCC, 2013

Figure 6.20: A synthesis of the magnitude of biogeochemical feedbacks on climate. Gregory et al. (2009) proposed a framework for expressing non-climate feedbacks in common units ($W\ m^{-2}\ K^{-1}$) with physical feedbacks, and Arneth et al. (2010) extended this beyond carbon cycle feedbacks to other terrestrial biogeochemical feedbacks. The figure shows the results compiled by Arneth et al. (2010), with ocean carbon feedbacks from the C4MIP coupled climate-carbon models used for AR4 also added. Some further biogeochemical feedbacks are also shown but this list is not exhaustive. Black dots represent single estimates, and coloured bars denote the simple mean of the dots with no weighting or assessment being made to likelihood of any single estimate. There is *low confidence* in the magnitude of the feedbacks in the lower portion of the figure, especially for those with few, or only one, dot. The role of nitrogen limitation on terrestrial carbon sinks is also shown — this is not a separate feedback, but rather a modulation to the climate-carbon and concentration-carbon feedbacks. These feedback metrics are also likely to be state or scenario dependent and so cannot always be compared like-for-like (see Section 6.4.2.2). Results have been compiled from (a) Arneth et al. (2010), (b) Friedlingstein et al. (2006), (c) HadGEM2-ES (Collins et al., 2011) simulations, (d) Burke et al. (2012), (e) von Deimling et al. (2012), (f) Stocker et al. (2013). Note the different x-axis scale for the lower portion of the figure.

Uendret klima,
høyere CO2

Varmere klima,
uendret CO2

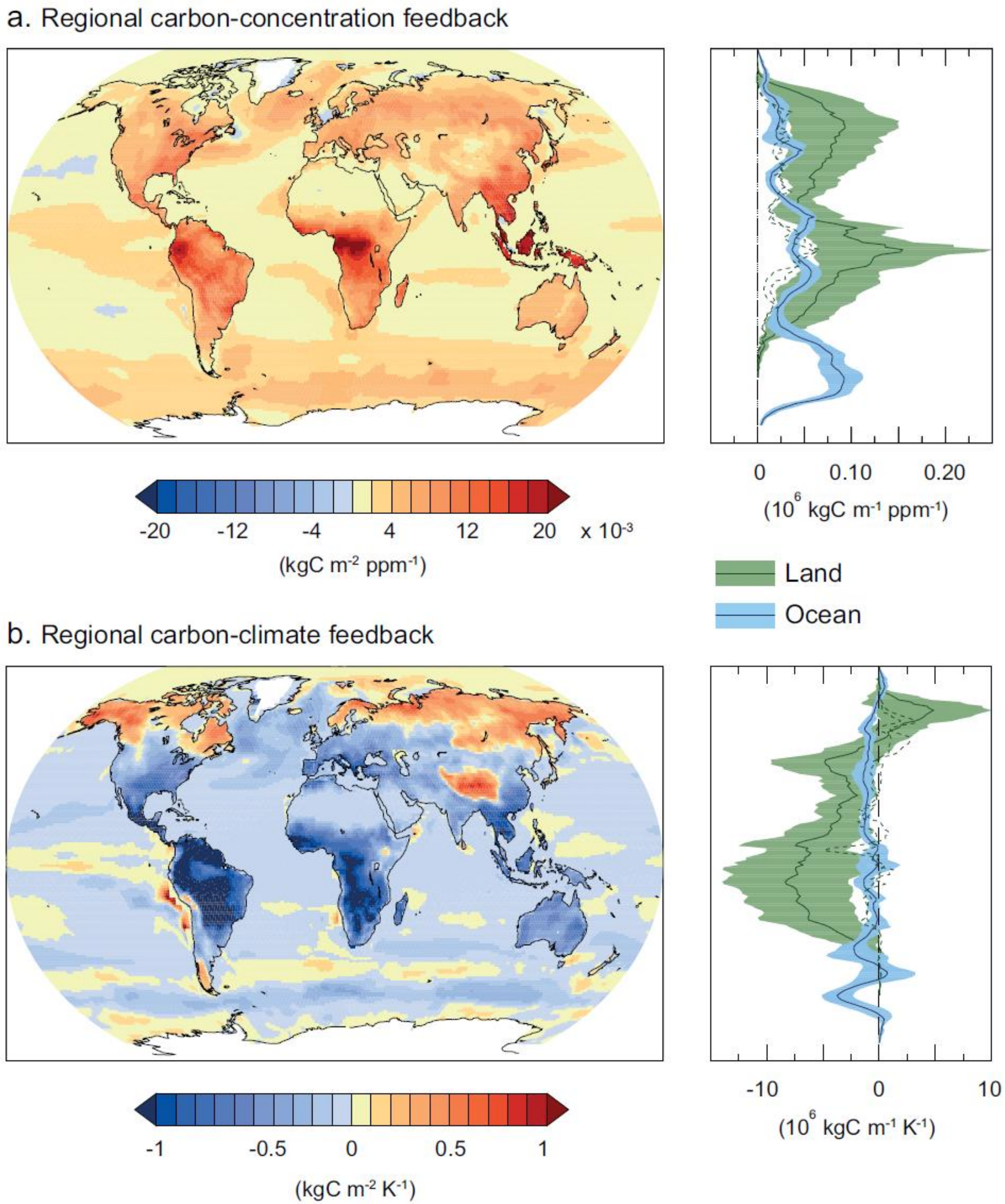

Mer CO_2 i atmosfæren
➔ høyere opptak i hav og på land

Høyere temperatur
➔ høyere/lavere opptak i hav og på land

Figure 6.22 | The spatial distributions of multi-model-mean land and ocean β and γ for seven CMIP5 models using the *concentration-driven* idealised 1% yr^{-1} CO_2 simulations. For land and ocean, β and γ are defined from changes in terrestrial carbon storage and changes in air–sea integrated fluxes respectively, from 1 × CO_2 to 4 × CO_2, relative to global (not local) CO_2 and temperature change. In the zonal mean plots, the solid lines show the multi-model mean and shaded areas denote ±1 standard deviation. Models used: Beijing Climate Center–Climate System Model 1 (BCC–CSM1), Canadian Earth System Model 2 (CanESM2), Community Earth System Model 1–Biogeochemical (CESM1–BGC), Hadley Centre Global Environmental Model 2–Earth System (HadGEM2–ES), Institute Pierre Simon Laplace– Coupled Model 5A–Low Resolution (IPSL–CM5A-LR), Max Planck Institute–Earth System Model–Low Resolution (MPI–ESM–LR), Norwegian Earth System Model 1 (Emissions capable) (NorESM1–ME). The dashed lines show the models that include a land carbon component with an explicit representation of nitrogen cycle processes (CESM1-BGC, NorESM1-ME).

Er det ikke slik at CO_2 allerede er så høy at all stråling som kan absorberes blir absorbert ➔ Økning vil ikke påvirke energibalansen?

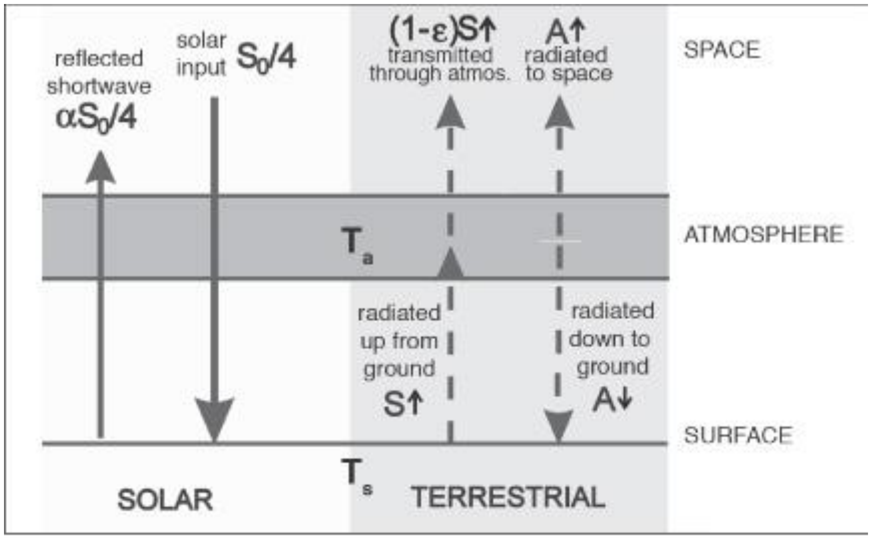

Figure 2.8: A leaky greenhouse. In contrast to Fig. 2.7, the atmosphere now absorbs only a fraction, ε, of the terrestrial radiation upwelling from the ground.

Strålingen $A\uparrow$ til verdensrommet er gitt ved $A\uparrow = \varepsilon\sigma T_a^4$ (Likning 2.14)

Mer CO_2

➔ strålingen kommer fra et nivå høyere oppe

➔ T_a redusert

➔ mindre stråling til verdensrommet

➔ netto oppvarming av atmosfæren

➔ T_a øker

➔ ny energibalanse

➔ økt overflatetemperatur T_s

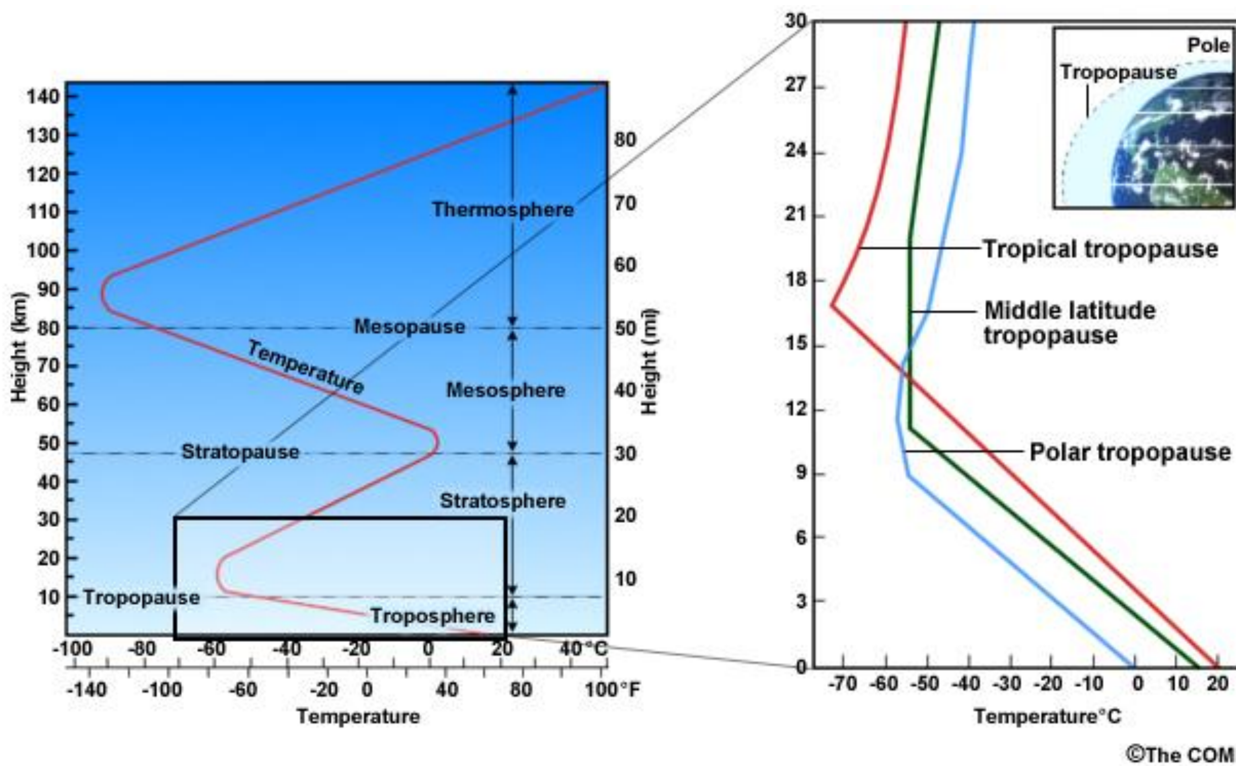

Varmekraftverk basert biobrensel og CCS: En mulighet for negative CO_2 utslipp?

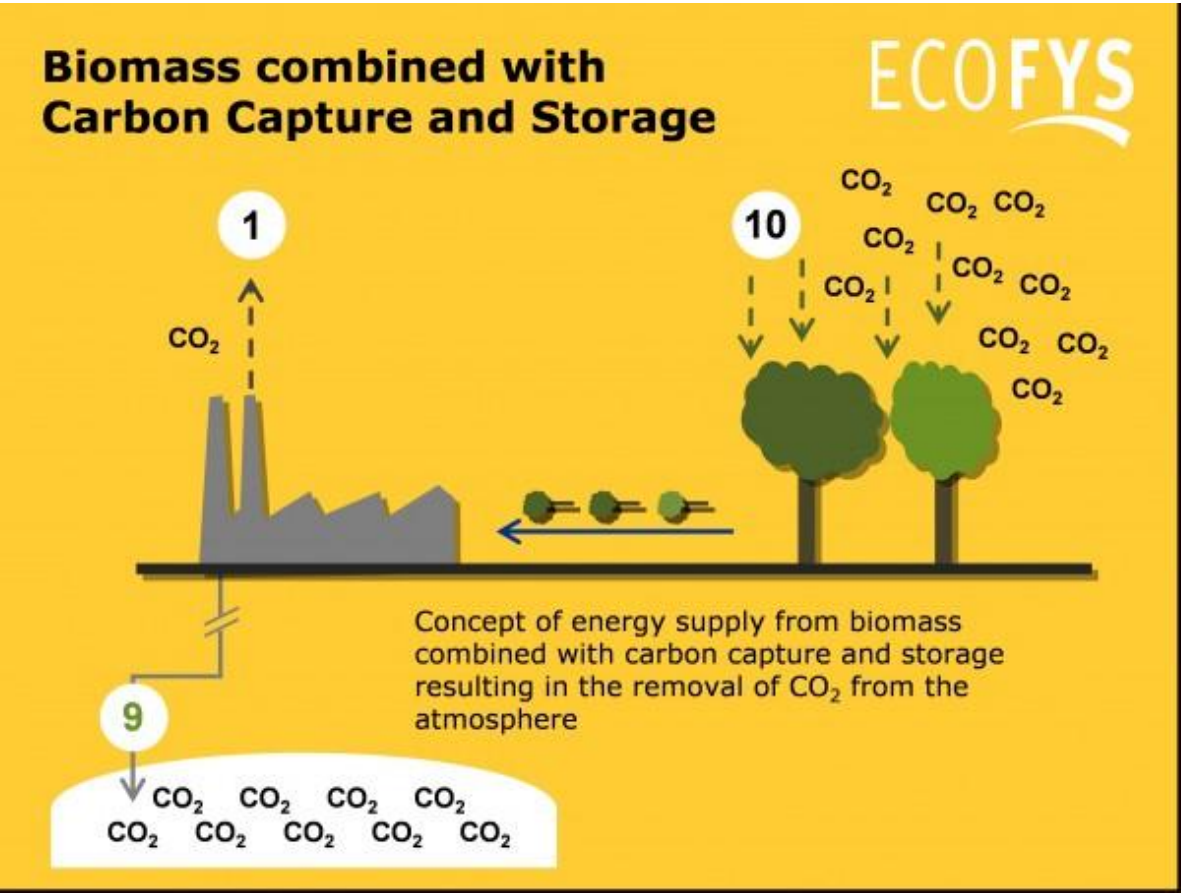

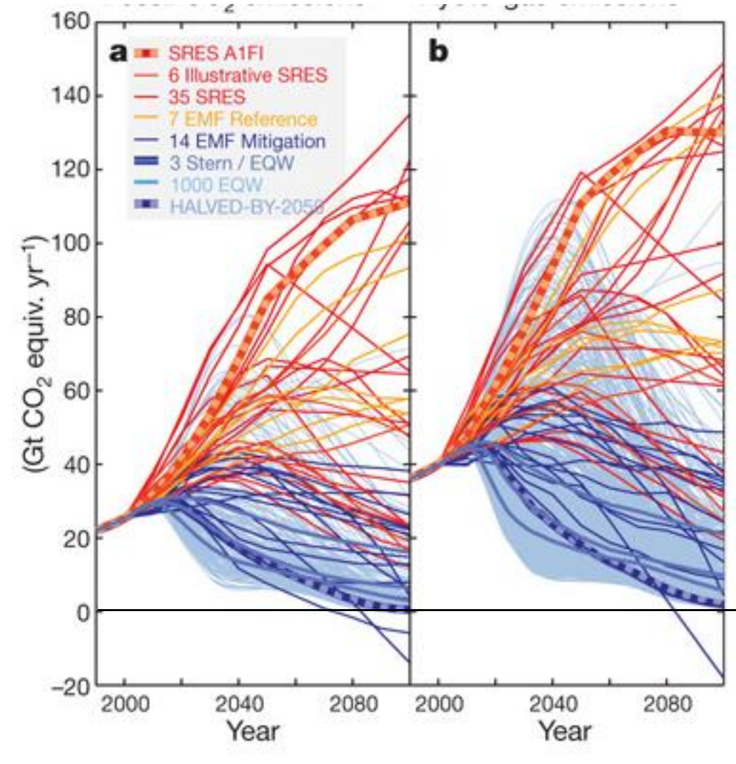

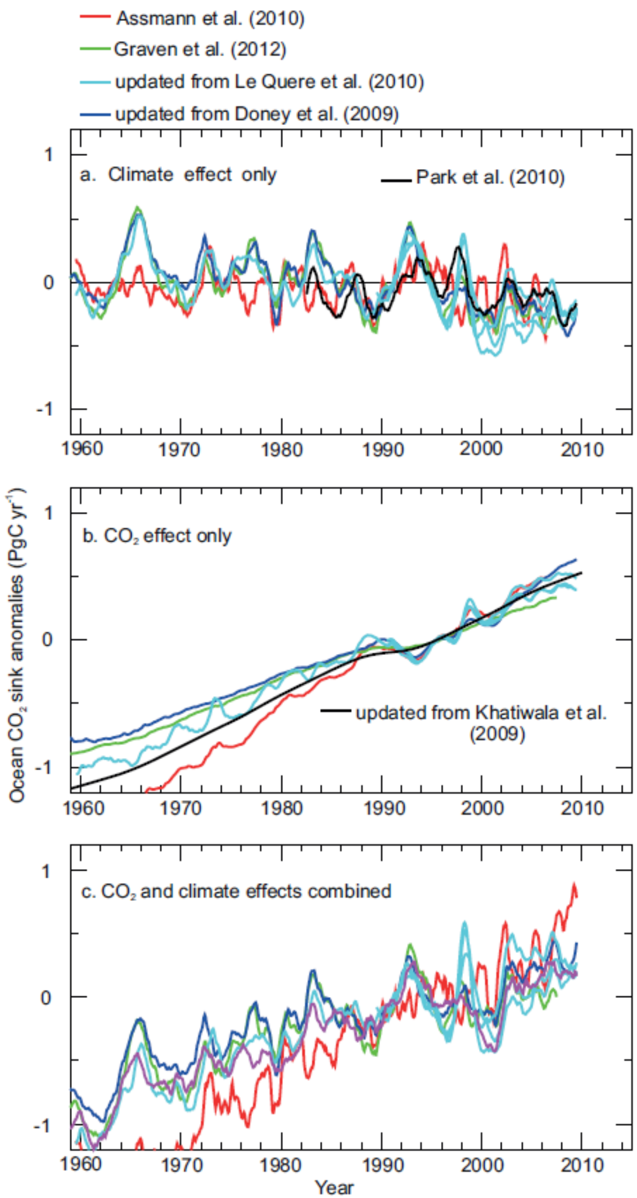

Figure 6.14 | Anomalies in the ocean CO_2 ocean-to-atmosphere flux in response to (a) changes in climate, (b) increasing atmospheric CO_2 and (c) the combined effects of increasing CO_2 and changes in climate (PgC yr^{-1}). All estimates are shown as anomalies with respect to the 1990–2000 averages. Estimates are updates from ocean models (in colours) and from indirect methods based on observations (Khatiwala et al., 2009; Park et al., 2010). A negative ocean-to-atmosphere flux represents a sink of CO_2, as in Table 6.1.

Bidrag til CO2-opptaket i havet.